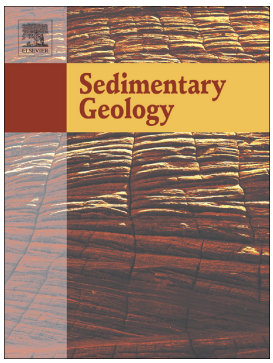

Effect of aragonite to calcite transformation on the geochemistry and dating accuracy of speleothems. An example from Castañar Cave, Spain

Rebeca Martín-García, Ana M. Alonso-Zarza, Silvia Frisia, Álvaro Rodríguez-Berriguete, Russell Drysdale, John Hellstrom

PII: S0037-0738(19)30025-9
DOI: https://doi.org/10.1016/j.sedgeo.2019.01.014
Reference: SEDGEO 5446

To appear in: *Sedimentary Geology*

Received date: 1 October 2018
Revised date: 29 January 2019
Accepted date: 30 January 2019

Please cite this article as: R. Martín-García, A.M. Alonso-Zarza, S. Frisia, et al., Effect of aragonite to calcite transformation on the geochemistry and dating accuracy of speleothems. An example from Castañar Cave, Spain, Sedimentary Geology, https://doi.org/10.1016/j.sedgeo.2019.01.014

Effect of aragonite to calcite transformation on the geochemistry and dating accuracy of speleothems. An example from Castañar Cave, Spain

Rebeca Martín-García[1,2], Ana M. Alonso-Zarza[2], Silvia Frisia[3], Álvaro Rodríguez-Berriguete[2], Russell Drysdale[4,5], John Hellstrom[6]

[1]Station d'Ecologie Théorique et Expérimentale - UMR 5321 CNRS. 09200 Moulis, France. rebeca.martingarcia@sete.cnrs.fr

[2]Departmento de Mineralogía y Petrología, Facultad de Ciencias Geológicas, Instituto de Geociencias CSIC, UCM, 28040 Madrid, Spain.

[3]School of Environmental and Life Sciences, The University of Newcastle, Callaghan NSW 2308, Australia.

[4]School of Geography, University of Melbourne, VIC 3010, Australia

[5]Laboratoire EDYTEM - UMR 5204 CNRS, Université Savoie Mont Blanc, 73376 Le Bourget du Lac Cedex, France

[6]School of Earth Sciences, The University of Melbourne, VIC 3010, Australia

ABSTRACT

Aragonite speleothems are increasingly being used as high-resolution climate proxies; however, aragonite is unstable and susceptible to diagenetic transformation into calcite leading to mineralogical, textural and geochemical alterations that have not been fully investigated. To provide some insights to these modifications, this study combines stable isotope geochemistry and U-series dating with petrological observations and EMPA elemental analyses to characterize a stalagmite from Castañar Cave (Cáceres, Spain) that shows primary aragonite diagenetically altered and with reverse ages. The diagenetic processes include recrystallization to calcite, micritization and dissolution. Characterization and interpretation of the chemistry and nature of the waters from which

the aragonite precipitated, and of the ones that subsequently formed the calcite, indicates that both polymorphs formed from the same fluids. These fluids hydrochemically evolved from an “aragonite mode” to a “calcite mode” along a diagenetic path within the sample. The results show that during transformation the system stayed close in one of the stages, and open in the other with the same textural result. Reverse ages are found either in the recrystallized areas or in the primary aragonite, caused by two different U-remobilization mechanisms, U-leaching due to flowing waters on the surface, and U-loss during the transformation process. These results highlight the complex behavior of speleothems during diagenesis and the impact on the geochemical information of the primary and secondary phases, and thus the importance of petrological and geochemical characterization of speleothems for paleoclimatic studies.

Keywords: speleothems, aragonite, calcite, diagenesis, U/Th dating, geochemistry

1. Introduction

Speleothem-based studies targeted to decipher past climate eventsand the rates at which they occur rely on accurate dating (Drysdale et al., 2009; St Pierre et al., 2009). The U-series dating method is well-known for dating quaternary carbonates up to ca. 500,000 years (Frank et al., 2000; Hellstrom, 2003; van Calsteren and Thomas, 2006). This method has been widely used in combination with other geochemical analyses (major and minor elements, stable isotopes, etc) to obtain paleoclimate information (Kaufman 1998; Fairchild et al., 2006; Spötl et al., 2008).

There is secular equilibrium between U and Th isotopes in the host rock, which usually is at least several million years old. However, this secular equilibrium is not present in the percolation waters due to the different geochemical behavior of both elements. Th is insoluble and therefore the ratio $^{230}Th/^{238}U$ in drip water is 0, whereas the U concentration in drip waters is well above the equilibrium value because ^{234}U is very soluble (Scholz and Hoffmann, 2008), this is one of the bases of this dating technique. Initial $^{234}U/^{238}U$ in drip waters can vary greatly depending on age of the host rock and time of residence of water in the rock. In any case this does not affect the reliability of the U/Th-series dating technique since the initial $^{234}U/^{238}U$ ratio is not necessary for the calculations (Scholz and Hoffmann, 2008).

However, in some cases U/Th analysis indicates inverted ages for the speleothem layers, which would seem to disqualify the dating since the most important criterion for accepting an age as correct is its accordance with stratigraphic order, where oldest layers underlay younger ones (Kaufmann 2003; Romanov et al. 2008).

Diagenetic transformation of speleothems composed of unstable phases, such as Mg-rich calcites and aragonite, can alter the chemical properties of the deposit and it is a critical issue for the accuracy of dating. In most cases, transformation from a precursor to a stable phase is clearly indicated by changes in the fabric of the speleothem (Frisia, 1996; Woo and Choi, 2006; Martín-García et al., 2009; Perrin et al. 2014; Frisia et al, 2015). There is, however, the possibility that topotactic diagenetic transformations preserve the initial precursor fabric (Frisia-Bruni and Wenk, 1985; Bajo et al. 2016), or that the transformation itself proceeds through crystalline defects and initiates at the core, rather than in the outer layer of the stalagmite (cf. Frisia et al., 2002). This last case is particularly important, because the ages of the transformed phase may not mark the occurrence of mineral transformation, but rather other diagenetic phenomena such as

U (or Th) leaching. U (or Th) remobilization could indicate that there has been remobilization of other chemical species as well, and so transformed aragonite to calcite speleothems should be treated with caution. The simple calculation of the amount of aragonite not transformed in a sample used to normalize chemical data would be, in the case of remobilization, not correct (Ayliffe and Veer, 1988).

In this study we analyzed a stalagmite from Castañar Cave clearly affected by digenesis, characterized by a mosaic calcite core and aragonite cortex, in order to understand, first the carbonate diagenetic processes, secondly the effects of diagenesis on the geochemical behavior of the different elements and stable isotope values, and finally the impact that this behavior has on the age data.

2. Cave setting

Castañar Cave is located in Extremadura (Spain) (39º37'40''N, 5º24'59''W, 590 m.a.s.l.), in the southern part of the Iberian Massif (Fig. 1.A). The climate of the area is mild continental with Mediterranean influence, with a mean annual temperature of about 16ºC, annual thermal oscillation of about 20ºC, and precipitation with pronounced interannual and seasonal variability. The mean annual rainfall of 750 mm falls mainly in winter (Ninyerola et al. 2005). Vegetation above the cave consists mostly of olive trees and Mediterranean oak. Soils are strongly eroded due to the deforestation caused by agriculture (Delgado-Tejeda, 1988).

The cave is hosted in the Neoproterozoic rocks that form the core of the Ibor anticline (Fig. 1.B). These rocks, shales and greywackes with interbedded dolostones and magnesites, formed close to the Neoproterozoic–Cambrian boundary (Alonso-Zarza et al., 2011). Dissolution of the dolomitic and magnesitic beds and extensive weathering

of shales and greywackes led to the collapse of the ceilings, creating and enlarging the cave. Speleothems in the cave vary in their mineralogy and morphology in accordance with hostrock litho-types. Dominant speleothem-forming minerals are generally aragonite and calcite, but moon-milk deposits and crusts are composed by Mg-rich carbonates such as dolomite, huntite, magnesite and hydromagnesite (Alonso-Zarza and Martín-Pérez, 2008).

Dissolution of dolomite and magnesite influences the chemistry of cave watersthat is characterised by high Ca^{2+} (~38 mg/l), Mg^{2+} (~18 mg/l in drip waters and ~34 mg/l in pools) and HCO_3^- (~210 mg/l) (Garcia-Guinea et al., 2013). The Sr^{2+} content is less than 0.1 mg/l. The Ca/Mg ratios vary from 0.5 to 1.0 mol/mol. Castañar Cave is a "low energy cave" (Fernández-Cortés et al., 2011) with very high microenvironmental stability throughout the annual cycle under natural conditions. It has an outstanding concentration of ^{222}Rn, with an annual average of 32246 Bq/m^3 (Lario et al., 2006), much higher than the average 2500 Bq/m^3 concentration in most of the caves studied around the world (Hakl et al., 1997; Cigna, 2005). The source of this radonare the radioactive nuclides of Ac, Th and U-decay series present in the host rock. According to García-Guinea et al. (2013), during the leaching of the host rock, the nuclides concentrate in the hydrous silica deposits that cover the surface of some parts of the cave, including the aragonite ceiling crusts, showing similar radionuclide elements than the host rock but in higher concentrations.

At present, there is no flowing water in the cave, although there are small pools and drips in some areas and capillary seepage water flow has been observed in all rooms. However, previous studies have individuated another source of fluid in condensation, which contributed to the complexity of meteoric diagenesis resulting in micritization and neomorphism that collectively modify speleothem mineralogy and textures (Martín-

García et al., 2009; Martin-Pérez et al., 2012). Cave temperature is at a relatively constant value of 17 ± 0.09ºC, which reflects the mean annual temperature at surface. The annual CO_2 concentration values in the cave atmosphere are 3680 ± 1120 ppm (Sánchez-Moral et al. 2006). Relative humidity is higher than 99.5%, close to saturation (accuracy ±0.03ºC and ±0.6%) (Fernández-Cortés et al. 2010).

3. Methods

Stalagmite COR-2 was sampled at -20 m from the surface, in a square cross section gallery with very steep walls and controlled by a normal fault. COR-2 was formed in a slope that connects this gallery with a lower chamber (Fig. 1.C). It is composed of aragonite and calcite. Due to its fragility, the sample was embedded in a resin containing Epofer EX 401 and Epofer E 432 in a vacuum system. Thin sections were then cut along the vertical growth axis and examined by standard optical microscopy in both plane-polarized and cross-polarized light.

Scanning Electron Microscope observations were carried out at a JEOL 6400 electron microscope working at 20 kV equipped with secondary electron and backscattered electron detectors and with energy dispersive X-Ray analyser for semi-quantitative element compositions.

Quantitative Ca^{2+}, Mg^{2+}, Sr^{2+}, Fe^{2+}, Mn^{2+} and Ba^{2+} concentrations in 109 points and 3 profiles of the sample, including all mineralogies and textures, were obtained by using an Electron Microprobe Analyser (JEOL JXA 8900 M) operating at 15 kV and 20 nA and employing an electron beam diameter of 5 μm. Resolution of the profiles was 10 μm.

Mineralogical characterization of 7 samples form COR-2 was performed by X-ray diffraction using a Philips PW-1710 XRD system operating at 40 kV and 30 mA, at 2º/min from 2-66º 2θ, with monochromatic CuKα radiation.

42 powder samples for stable isotopes were collected along the central growth axis of the stalagmite at increments of 0.25 to 0.5 mm, and 73 transversal from the core to the surface at increments of 0.25 mm. Powders were then analyzed on a GV2003 continuous-flow isotope ratio mass spectrometer at the Department of earth Sciences, University of Newcastle, Australia. Conventional acid-digestion was carried out by using the analytical protocols outlined in Drysdale et al. (2009). The mean 1s analytical reproducibility of a Carrara Marble internal working standard (NEW1) is 0.05‰ for $\delta^{13}C$ and 0.09‰ for $\delta^{18}O$. Stable carbon and oxygen isotopic ratios are reported in ‰, relative to the Vienna Pee Dee Belemnite (VPDB) and the Standard Mean Ocean Water (SMOW) scales using the standard notation.

U/Th dating was carried out on 7 samples of COR-2. The samples were collected following the growing axis and selecting all of the mineralogies and fabrics present in the stalagmite. 5 to 100 mg of sample was drilled from the speleothems with a dental drill andthe radiometric analysis was done by a Nu Instruments multi-collector ICP-MS at the School of Earth Sciences of the University of Melbourne using the procedure described by Hellstrom (2003).

4. Results

4.1. Stalagmite description and petrography

Candle-shaped stalagmite COR-2, formed on top of a flowstone in the Corales room (Fig. 1.C) and is 21 cm long, with a diameter of 5 cm. When collected *in situ*, the

stalagmite was not fed by dripping. The outer surface appeared to consist of an array of needle-crystals coated by a brownish stain, most likely related to the adsorption of clay onto the crystals of a speleothem that had become inactive (Fig. 1.D). Stalagmite macroporosity appears to be low except at the tip of the speleothem, where pores developed in the direction of the crystal growth, with a maximum size of 0.5x1 mm.

The stalagmite architecture (Fig. 2), as seen when cut along the vertical growth axis consists of fabrics composed of diverse mixtures of aragonite and calcite (Fig. 3). These fabrics and mineralogies will be described in the following sections.

Elongated columnar aragonite crystals

Aragonite fabric forms the outermost part of the speleothem as a continuous rim, plus an internal zone resembling the same shape as the modern tip (fabric 1 Fig. 2). The crystals are transparent elongated columnar crystals, from 2 to 8 mm long, 80% to 100% aragonite (Fig. 2.A). These elongated crystals are arranged forming an angle of circa 45º to the vertical axis of the stalagmite towards the bottom. This angle diminishes progressively moving upwards, towards the tip of the stalagmite where it becomes 0º and is parallel to the axis. Critically, the orientations of the elongated crystals in the inner part of the stalagmite is the same as the topmost layer, and the two layers merge on the flanks (Fig. 4.A). Crystal length varies from 2 to 8 mm, with the longer individual crystals at the tip of the stalagmite. Crystals are very clean and transparent and show square terminations. The length-to-width ratio of the crystals is > 6:1 and they show sweeping extinction thus can be considered elongated columnar according to Frisia and Borsato (2010). Small (≈15 μm) euhedral calcite crystals growing on aragonite surfaces have been observed by SEM, their phase confirmed by XRD analyses

(Fig. 3, Fig. 4.C). The crystals forming the tip of the speleothem show dissolution features, possibly leading to an overall increase in porosity (Fig. 4.D.). In the areas close to the calcite mosaic, aragonite is only partly dissolved.

Calcite mosaic

Calcite mosaic fabric has been observed in the core part of the stalagmite (fabric 2, Fig. 2) being constrained by aragonite crystals The mosaic is composed of euhedral and transparent crystals of calcite ranging from 0.2 to 10 mm with aragonite relicts (30-50%) (Fig. 2.B). Calcite mosaic consists of two distinct size-groups (Fig. 5.A). The first and most abundant consists of large euhedral and equant crystals with mean dimension of 5 mm (in diameter) and a maximum of 10 mm (in diameter) with sharp crystal contacts. The second size group consist of euhedral crystals ranging from 0.2 to 0.5 mm in dimension. The large crystals form the majority of the mosaic and the smaller crystals are concentrated at the aragonite contact, and to a lesser extent between the large crystals (Fig. 5.B).

Calcite mosaic fabric is characterized by the presence of acicular aragonite relicts as already observed in both marine and spelean aragonite transformation examples (Sandberg and Hudson 1983; Frisia et al., 2002; Frisia, 2015). As in most cases, also in COR-2 the relicts can be observed as square tipped needles within the calcite crystals passing from a calcite crystal to the adjacent following the direction of the aragonite crystals at the rim (Fig. 5.C). Relicts can be either predominantly textural (only the texture of the precursor mineral is preserved, but the "bulk" mineralogy corresponds to the secondary phase) or mineralogical (the primary phase is still preserved). According to bulk XRD and EMPA analyses, most relicts in COR-2 still consist of 35% to 50% aragonite (Fig. 3). The percentage of observable relicts can vary

drastically from one crystal to another. Within the same crystal, the nucleus of the calcite can be rich in relicts but the edges can be relict-free (Fig. 5D).

Microcrystalline aragonite

In the contact between the aragonite and the calcite mosaic, microcrystalline aragonite occur as patches up to 2.5 x 0.5 cm, or as a thin line of less than 1 mm in the boundary between the aragonite crystals and the calcite mosaic (fabric 3 Fig. 2.C) (Fig. 6A). Under the polarizing microscope, the mass of microcrystalline texture is formed by a mesh of crystals of less than 4 μm mixed with small aciculums of 0.1 to 1 mm long and a few microns wide (Fig. 6.B, C) oriented in the same direction as the elongated crystals of the rim. According to XRD this mass is 100% aragonite (Fig. 3) and under fluorescent light there is no presence of organic matter.

Growth stages of COR-2

Fabrics are arranged in the following two main stages of formation-transformation, which repeat twice along the stalagmite length (Fig. 7):

Stage 1: formation of a speleothem composed entirely of aragonite elongated crystals (fabric 3. Fig. 2). Modeling of the original length of this initial speleothem following the relict crystals, gives a length of 12.5 cm and width of 5 cm. At some point after the formation of the aragonite the calcite nucleation in the core partially transformed the aragonite and left relicts (fabric 2). This transformation affected the inner part of the stalagmite from the bottom up to a length of 7.5 cm and a width of 3.5 cm, restricting the aragonite to a rim. Microcrystalline aragonite (fabric 3) formation probably occurred soon after that of calcite. Possible mechanisms for the occurrence of these processes will be discussed later.

Stage 2: after this first stage new aragonite elongated crystals (fabric 1) grew in optical continuity with the precursor aragonites, forming an upper part with the same diameter and shape as that of the first stage. The length of the aragonite in this stage was 4.5 cm, giving a total length of around 20 cm to the entire stalagmite. As in the stage before, after aragonite formation, calcite started to nucleate and the subsequent advance of the recrystallization process partially transformed the aragonite leaving relicts and producing the aragonite rim with a calcite area of around 3x3 cm (fabric 2). Microcrystalline fabric, in this second stage, appears between secondary calcite and the aragonite of Stage 2 but also at Stage 1 – Stage 2 contact.

4.2.Geochemistry

Elemental analysis

We used an EMPA analyzer to determine the distribution of Ca^{2+}, Mg^{2+}, Sr^{2+}, Fe^{2+}, Mn^{2+} and Ba^{2+} in all the different mineralogies and fabrics.

Table I shows the average mol % of carbonate of each element recalculated from the oxide form given by EMPA. Sr^{2+}, Fe^{2+}, Mn^{2+} and Ba^{2+} carbonate values are near zero in all of the mineralogies and textures analyzed. The amount of Mg^{2+} distinguishes aragonite from calcite: while all aragonite textures (primary columnar, relicts and microcrystals) have ~ 0% mol $MgCO_3$, mean % mol $MgCO_3$ for the large calcite crystals is 0.12, reaching up to 1.07 in the smaller crystals (Table I, Fig. 8). This means that even though calcites from COR-2 are far from being HMC (defined as > 4% mol $MgCO_3$ by Chave, 1954, 1964), the difference in Mg^{2+} concentration is enough to distinguish between calcite and primary aragonite and, thus, verifies the relicts as evidence of a primary mineralogical phase.

Stable isotopes

Isotopic composition of COR-2 was measured along two profiles, the first following the growth axis in Stage 1b calcite area, with a resolution of 0.5 mm along the 3.9 cm profile length, and the second profile perpendicular to the axis, from core to surface, with a resolution of 0.25 mm along the 1.85 cm profile length.

The first profile transects a mosaic of large calcite crystals full of relicts of aragonite (Fig. 9). The isotopic composition along the profile has a mean $\delta^{18}O$ value of -5.03‰ VSMOW and a mean $\delta^{13}C$ value of -7.77‰ VPDB. Variations of both values along the axis are less than ±0.27‰ from the mean value, related to the amount of aragonite relicts.

In the second profile (Fig. 10), the first texture is the equant mosaic of secondary calcite with relicts. Values in this region are similar to those in the first profile. The range of values for $\delta^{13}C$ is -7.95 to -7.59‰ VPDB and for $\delta^{18}O$ is -4.80 to -5.80‰ VSMOW. As the profile approaches the small calcite crystals near the aragonite rim, values in $\delta^{13}C$ decrease to the lightest isotope value of -10.03‰ VPDB whereas $\delta^{18}O$ remains constant. In the aragonite rim, both $\delta^{13}C$ and $\delta^{18}O$ values are heavier than in the calcites, particularly with $\delta^{13}C$, which reaches up to -6.04‰ VPDB.

4.3.U/Th Dating

In order to provide a time frame for the diagenetic processes affecting COR-2, U-series dating on seven points selected along the vertical growth axis and including all the fabrics identified by optical microscopy were carried out (Fig. 11, Table II). Doubtful results were re-analyzed. Studying each growth stage separately, the results show that:

Stage 1: 3 points were dated, one in the calcite mosaic (1) very near a microcrystalline patch, with an age of 76 ± 0.8 ka. Aragonite was dated in 2 points (2 and 3), 1 cm apart, giving very similar ages in stratigraphical order of 49.7 ± 0.3 ka and 49.7 ± 0.6 ka.

Stage 2. Sample 4 was taken in the aragonite microcrystalline area, 3 mm above point 3, and is 48.5 ± 0.4 ka old. The calcite mosaic (5) shows an age of 47.3 ± 0.2 ka. Aragonite of the tip (7) is 195.3 ± 2.1 ka and 6 mm below, another dating of the aragonite (6) gave an age of 57.0 ± 0.4 ka.

Comparing these results with the stratigraphic observations and the diagenetic path, there were some inconsistencies: calcite that transforms the primary aragonite of Stage 1 is older than the aragonite itself; aragonite of the tip is the oldest in the speleothem; and while in Stage 1 aragonite takes 200 years to grow 1 cm (from point 2 to 3), in Stage 2 it takes 138 ka to grow almost the same length (from point 6 to 7).

5. Interpretation and discussion

5.1.Formation of aragonite

The first stage of the stalagmite growth is the formation of elongated columnar aragonite crystals. Although aragonite is the high temperature and pressure polymorph of $CaCO_3$, it is known to form at surface conditions in a variety of environments, from shallow marine to meteoric (Tucker and Wright, 1990). Formation of this mineral in caves has been widely reported (Hill and Forti, 1997; Frisia et al., 2002; Woo and Choi, 2006; Martín-García et al., 2014; Domínguez-Villar et al., 2016; Wassenburg et al., 2016; Alonso-Zarza et al., 2018). Controlling factors for aragonite precipitation in cave systems are complex, documented to depend on the interaction between pH, Mg/Ca ratio in the parent waters, saturation index (SI), and the drip site characteristics within a

single cave (de Choudenz-Sanchez and González, 2009; Wassenburg et al., 2012). Historically, presence of aragonite has been linked to high Mg/Ca ratios in parent waters (Cabrol, 1978; Fernández-Díaz et al., 1996, Frisia et al., 2002; McMillan et al., 2005; Fairchild and Treble, 2009) and in fact, aragonite is commonly found in caves formed in dolostone or dolomitic limestone, where the host rock is the primary source of Mg^{2+} (Frisia et al., 2002; Martín-García et al., 2009; Wassenburg et al., 2012; Martín-García et al., 2014; Perrin et al., 2014; Rossi and Lozano, 2016). Filipov (1990) found that aragonite forms when Mg/Ca in the parent waters is higher than 0.4. Moreover, high concentrations of Mg^{2+} as well as high Mg/Ca ratios in the waters seem to inhibit the precipitation of calcite (i.e. Zhang and Dawe, 2000; Denniston et al., 2000; de Choudens-Sánchez and González, 2009), via the "poisoning" of the growth sites on the calcite faces by Mg ions (Lipmann, 1973; Rowling, 2004). However, the Mg/Ca ratio alone is not the major controlling factor for aragonite formation. Aqueous $CaCO_3$ saturation appears to be more important than Mg/Ca ratios, as lower super-saturation states for $CaCO_3$ seem to favor aragonite formation (Ahn et al., 2005; de Choudens-Sánchez and González, 2009), whereas in other cases, aragonite precipitates in the presence of relatively high super-saturations (Holland et al., 1964; Denniston et al., 2000). Other controlling factors for aragonite are growth and CO_2 degassing rates (Fernández-Díaz et al., 1996; Jones, 2017), which are directly inter-related. According to Jones (2017), aragonite occurs in springs when there is rapid CO_2 degassing of waters, which results in a very high super-saturation, without high Mg/Ca ratio. In the case of fluids with low super-saturation, de Choudens-Sánchez and González (2009) demonstrate that high Mg/Ca ratios are needed for aragonite formation, otherwise calcite would precipitate.

In present day Castañar cave, waters are slightly supersaturated for both minerals, SI_{ar} is 0.27 and SI_{cc} is 0.47. Concentration of Mg in the waters is circa 40.0 mg/l, and the Mg/Ca = 0.48-1.0, which is related to long residence in dolomite host rock (Sánchez-Moral et al. 2006). These super-saturation values favor precipitation of aragonite and increase growth rate, as shown by Duan et al. (2012). Nevertheless the Mg/Ca ratio threshold for aragonite formation is 1.2 (Bajo et al., 2016), which is not reached in Castañar Cave waters**.** Taking into account that development of aragonite elongated columnar morphologies has been related to constant drip rates, relatively low super-saturations and Mg/Ca ≥ 0.3 in the dripwaters (Frisia and Borsato , 2010), and considering the relatively high growth rates calculated for Castañar aragonite speleothems ~140 mm/ka (Martín-García, 2012), it is likely that primary aragonite precipitation in COR-2 is mainly due to high CO_2 degassing rates, which also generated high growth rates, with the Mg/Ca ratio being a secondary factor. Aragonite is usually linked to dry conditions, in which the low fluid flow, the highevaporation rates and the highMg/Ca ratio of the fluids due to the residence times in the host rock, shifts the system from a "calcite" to an "aragonite" mode (Railsback et al., 1994; Denniston et al., 2000; Frisia et al., 2002; McMillan et al. 2005; Wassenburg et al., 2012). When primary aragonite and calcite alternate in the same speleothem, aragonite is commonly considered a paleoaridity indicator (Spötl et al., 2002; Csoma et al., 2006).

5.2.Aragonite-to-calcite transformation

Observations of thin sections show that the calcite crystals of COR-2 bear large amounts (≤50%) of aragonite relicts, undoubtedly a proof of its secondary origin (Fig. 3). Aragonite-to-calcite transformation has been described in caves (Spötl et al., 2002; Ortega et al., 2005; Woo and Choi, 2006; Martín-García et al., 2009; Alonso-Zarza et

al., 2011; Caddeo et al., 2011; Lachniet et al., 2012; Martín-Pérez et al., 2012; Zhang et al., 2014; Domínguez-Villar et al., 2017) leading to two main end products: columnar calcite and equant calcite mosaic. In some cases, the transformation preserves the original texture of the precursor crystals, giving a fabric consisting of columnar calcite indistinguishable from the aragonite (Perrin et al., 2014). In this case, the process can be called "neomorphism" according to Folk's definition (1965), as the diagenetic process in which the unstable polymorph (aragonite) transforms into the stable one (calcite) in the presence of water and preserves the original texture. The other common textural result of this process is what is found in COR-2, a transformation from elongated columnar aragonite crystals to a calcite mosaic with acicular relicts (Frisia, 1996; Woo and Choi, 2006; Domínguez-Villar et al., 2017).

The decay of the U/Th series provokes the direct ejection of α-particles (i.e. helium nuclei) that recoil the daughter nuclide in its opposite direction, causing damage (tracks) to the crystalline lattice (Neymark, 2011). The damage caused by these recoiled nuclei weakens the stability of aragonite and the tracks act as nucleation sites, so they enhance the possibilities of transformation into calcite. The high amounts of U in the host rock and speleothems of Castañar cave, as in COR-2 (Table II), can be linked to the abnormally high contents of Rn found in Castañar cave atmosphere (García-Guinea et al., 2013). This Rn is a product of the U/Th series decay, so it could be the case that the aragonite in COR-2 was weakened during the emission of α-particles making it even more metastable and prone to transformation into calcite. Nevertheless more studies should be done in this direction to confirm the hypothesis In COR-2, SEM observations show rhombohedral microcrystals of calcite growing on the aragonite elongated c faces (Fig. 4.C) being probably the first stage of transformation. Subsequently these crystals continued growing and engulfed aragonite fibers. Frisia et al. (2002) and similarly Woo

and Choi (2006) described the transformation as induced by the presence of prior calcite crystals among aragonite needles, favoring the nucleation of diagenetic calcite. As the transformation process occurred only in inner parts of the stalagmite nucleation sites are difficult to determine and probably simultaneously at different sites. Fluid must have migrated from the speleothem surface to diagenetic sites through microporosity/permeability of the aragonite crystals. In this scenario, any small change in the physicochemical composition of the fluids that are in the limit between aragonite and calcite, would lead to a change in mineral precipitation. Migrating fluid hydrochemistry must be different from that of fluids from which aragonite precipitated. A higher saturation index with respect to calcite, or a lower Mg/Ca ratio could lead to the nucleation of calcites. Usually, periods of less evaporation in cave environments related to wetter conditions have been related to a change from aragonite to calcite in the mineral phases that precipitated in the same speleothem (Denniston et al., 2000). This explanation is based on the fact that Mg/Ca ratio decreases with increasing water supply, thus removing Mg inhibition of calcite precipitation.

Transformation of aragonite to calcite, a wet transformation process, takes place along a thin 100 Å to 1 µm film of fluid (Pingitore, 1976). It forms an interface in which aragonite dissolves on one surface and calcite re-precipitates on the other surface simultaneously (Perdikouri et al., 2008). Precipitation of calcite generates local aragonite supersaturation, leaving undissolved relicts. The acicular morphology of the relicts and their disposition, parallel to the columnar crystals, suggests a crystallographic control on the aragonite dissolution. Splitting surfaces observed on the columnar crystals could have acted as preferred dissolution surfaces. This process does not change major element content (Ca, C, O), but results in a depletion in Sr^{2+} and an enrichment in Mg^{2+} of calcites with respect to aragonite (Frisia et al., 2002; Martín-

Pérez et al., 2012). According to Perrin et al. (2014) this is an open-system reaction that releases Sr^{2+} from the dissolving aragonite, while calcite incorporates a certain amount of this Sr^{2+} and Mg^{2+} from the fluid. Differences in Mg^{2+} content in the growing bands of each particular calcite crystal (Fig. 9, 10) reflect a fine-scale precipitation of calcite during the transformation process. This suggests a modification of the parent fluids during a complex pattern of diagenetic changes, which involve a mechanism similar to Prior Calcite Precipitation (PCP) (Fairchild and Treble, 2009; Baker et al., 2016) within the same stalagmite, that locally increases the Mg/Ca ratio and removes Sr^{2+} from the system. Overall, the system was open, but water recharge in the pores of the speleothem inner parts was not fast enough to prevent local fluid enrichment in Mg^{2+}, suggesting that fluid flow within the stalagmite was slower than the transformation rate. Such mechanism would lead to a geochemical evolution of the fluids as the different mineral phases precipitate.

The oxygen and carbon isotope pattern indicates mean compositions of the secondary calcite crystals is 0.16‰ lighter for the $\delta^{18}O$ and 0.53‰ lighter for $\delta^{13}C$ with respect to aragonite. Specifically, smaller calcite crystals have the lightest mean values for $\delta^{13}C$, differing 1.41‰ from the aragonite mean values and 0.88‰ from the large calcite crystals mean values (Fig. 10). Theoretically, fractionation factor between both minerals co-precipitating at 25º is between 0.6 and 0.8‰ for $\delta^{18}O$ (Kim et al., 2007) and between 1.4 and 1.8‰ for $\delta^{13}C$ (Romanek et al., 1992). Low variation of the large calcite crystals and the aragonite isotopic values supports the idea of both minerals precipitating from the same or very similar solution. For the small calcites, the lighter values in $\delta^{13}C$ corroborate the hypothesis of the evolving fluids. If these calcite crystals are the last mineral phase to form, they should have formed from waters that are

enriched in the light C isotope, as the minerals tend to incorporate the heavier counterpart for lattice stability (Hoefs, 2009).

Aragonite to calcite transformation in speleothems has been addressed as a process that involves the presence of more diluted waters, either related to climate change or to changes in the local hydrology of the cave, percolating into the speleothem via the porous system (Frisia et al., 2002; Woo and Choi; 2006; Lachniet et al., 2012; Domínguez-Villar et al., 2017). However data obtained from COR-2 suggests that the transformation can occur without the addition of external waters to the system, thus precipitating calcite from the same fluids from which aragonite precipitated in the first place, after a complex diagenetic evolution (Fig. 12). Fluids would precipitate aragonite, which extracts Ca from the system, increasing the Mg/Ca ratio and decreasing the SI_{ar}. In this scenario, theoretically, calcite would be unlikely to precipitate due to the Mg/Ca ratio value, probably above the threshold of aragonite (1.2). However, Rodríguez-Berriguete et al., (2018) showed that in travertines formed from cool meteoric waters with Mg/Ca between 2.0 and 10.0 mol/mol, aragonite precipitates near the spring, at high degassing rates, while calcite starts to form downstream in less turbulent conditions. Analogously, absence of degassing processes in pores of COR-2 would trigger precipitation of calcite. These calcites would grow and transform the aragonite, incorporating Ca^{2+} and thus increasing the Mg/Ca ratio of the remnant fluids. Microscopy observations suggest that the small calcite crystals are the last to form in the transformation process. According to the elemental analyses, they have the highest Mg^{2+} content of all the mineral phases (Fig. 8). This supports the idea of such diagenetic evolution of fluids, and their smaller crystal size can be related to the poisoning by Mg^{2+}, which causes the calcite to grow smaller (Folk, 1974). In this case, even if cave waters where continuously in an “aragonite mode”, the fluids inside the speleothem

could have change to "calcite mode", so the transformation could have started in the inner parts at the same time as aragonite was still precipitating on the surface.

5.3.Formation of microcrystalline aragonite

In COR-2, microcrystalline texture always appears related to semi-dissolved aragonite fibers. Textural evidence strongly suggests that microcrystalline aragonite formed only from the modification of the texture of the columnar elongated aragonite crystalsand not as a primary precipitate (Fig. 6.B) or as a biologically induced product. Elemental analyses of this texture support this origin; there are no differences in composition between the columnar crystals and the microcrystals (Table I). Such texture is commonly found in local patches at the contact with original aragonite and mosaic of secondary aragonite-bearing calcites; no biogenic features have been found. Martín-García et al. (2011, 2014) described this texture in aragonites as the result of an unfinished dissolution process that caused the disaggregation of crystals rather than their complete disappearance. If this were the case, the process can be called "micritization" and it would be a pure diagenetic process, as defined by Reid and Macintyre (1998), a process of destruction of the original structure of a carbonate leading to formation of microcrystalline textures.

In caves, a similar texture forms as a product of condensation corrosion/weathering on the surfaces of the speleothems by corrosive waters (Auler and Smart 2004; de Freitas and Schmekal 2006; Martín-García et al. 2009; Martín-García et al., 2011; Domínguez-Villar et al., 2016). In COR-2 these areas of microcrystalline aragonite do not seem to reflect a previous surface, but the association with pervasive micro porosity may indicate the relation of this microcrystalline aragonite with the

dissolution of the preexisting aragonite crystals related to the action of undersaturated (i.e. aggressive) waters.

Position of microcrystalline patches between calcite mosaic and fresh aragonite columnar crystals suggests an origin related with the same fluids that cause transformation from aragonite to calcite, when the fluids are no longer saturated with respect to calcite (or aragonite) and start dissolving the aragonite crystals, leaving pores and semi-dissolved/micritized crystals (Fig. 12).

5.4.Theoretical calculations of temperature and stable isotopes

Temperature was calculated using the Coplen's (2007) equation for oxygen isotope fractionation between calcite and water:

$1000*\ln\alpha_{cc\text{-}w} = \delta^{18}O_{cc}\text{-}\delta^{18}O_w = 17.4*(1000/T)\text{-}28.6$

where $\delta^{18}O_{cc}$ is the mean isotope signal of COR-2 calcite, and that of $\delta^{18}O_w$ is assumed to be the average value from Castañar cave waters: -6.20‰ (VSMOW) (Sánchez-Moral, 2015).

Water temperature was estimated assuming isotopic fractionation of calcite-water is not different from that of aragonite-water. Calculated temperatures range from about 14°C to 19°C, 3-5°C lower for aragonite than for calcite. Therefore, if $\delta^{18}O_w$ had been constant throughout time, and there had been no differences in isotope fractionation between calcite and aragonite, then periods of aragonite precipitation were 3-5°C colder than those occurring during calcite precipitation. However aragonite and calcite $\delta^{18}O$ values are clearly different (Fig. 10). The differences of the average $\delta^{18}O$ values of calcites and aragonites (0.7 to 0.94‰) were used to make corrections to

aragonite samples, by subtracting those differences from Coplen's (2007) equation. These calculations give similar temperatures for calcite and aragonite, ranging from 17 to 19ºC. As a consequence, $\delta^{18}O$ and T can be assumed to be constant throughout time, and the different isotopic values of calcite and aragonite are due to the different fractionation relative to water of each polymorph. However, this assumes that both aragonite and calcite precipitated from the same waters. This result supports the idea of an initial aragonite-precipitating fluid evolved during diagenesis to a calcite-precipitating fluid, with no significant $\delta^{18}O_w$ or temperature changes.

Theoretical δ^{18}Ow values for both minerals forming from today waters were also calculated using Coplen's (2007) equation at a temperature of 17.8°C, the mean value of temperature measured in Sánchez-Moral (2015). As with temperatures, it was initially assumed that there is no difference in isotope fractionation between calcite and aragonite, so $\delta^{18}O_w$ values were calculated without applying aragonite corrections. In this case the results indicate that temperature and/or $\delta^{18}O_w$ changed throughout time. In fact, a difference of 0.7‰ in oxygen isotope fractionation accounts for a difference of about 3°C. In this study most of the corrections applied to aragonite are > 0.7‰, so temperatures may differ by more than 3°C. However, the effects of such variation of temperature would be smaller if accompanied by a slight increase in $\delta^{18}O_w$. After correction for aragonite samples, $\delta^{18}O_w$ calculated for both polymorphs was similar, between -6.2 and -6.4‰ (VSMOW), so during speleothem formation, temperature and/or $\delta^{18}O_w$ remained close to constant.

Temperature andpH measurements and isotope analyses of waters from Castañar Cave were used to calculate the expected isotope signals of calcite and aragonite formed from these waters. $\delta^{18}O_{cc}$ was calculated using Coplen's (2007) equation, and $\delta^{18}O_{ar}$ by adding 0.7‰. For $\delta^{13}C$ it was assumed that all DIC (dissolved organic carbon) was

HCO_3^- (pH is about 7 or slightly higher), so first the $\delta^{13}C$ of CO_2 was calculated (Mook, 1974), and then equations for aragonite and calcite $\delta^{13}C$ by Romanek et al. (1992) were applied using the mean value of -16.83‰ for the $\delta^{13}C_{DIC}$ from one of the cave lakes (Sánchez-Moral, 2015). For the mean temperature of 17.8°C (Sánchez-Moral, 2015), the expected isotope signal (referred to VPDB standard) for calcite precipitated from these waters is -5.01‰ for $\delta^{18}O$ and -6.99‰ for $\delta^{13}C$, whereas for aragonite the expected isotope signal is -4.33‰ for $\delta^{18}O$ and -5.27‰ for $\delta^{13}C$. This means that these theoretical calcites would have heavier isotope signals than the measured ones, and theoretical aragonite would have similar to slightly heavier $\delta^{18}O$ and heavier $\delta^{13}C$ than the aragonite from COR-2. Consequently, during speleothem formation and subsequent diagenetic changes aragonite and calcite from COR-2 probably precipitated from waters with T > 17.5 °C, and $\delta^{18}O_w$ < -6‰ (VSMOW), values slightly different from the present.

5.5.Problems with U-series

U is transported by water from soil and host rock to speleothems as the U(VI) aqueous species are highly mobile. In meteoric waters the ion UO_2^{2+} dominates, strongly tending to couple with various anions common in natural waters, especially CO_3^{2-}. The structure of the $UO_2(CO_3)_3^{4-}$ unit in the aqueous form is incorporated in the aragonite almost intact, while in calcite, the unit undergoes structural disruption (Reeder et al., 2000). This causes a preferential incorporation of U(VI) in aragonite with respect to calcite. Dated samples from COR-2 give an amount of U ranging from 1.4 to 14µg/g, which is above the 0.1–1µg/g average content of U in cave carbonates (Quinif, 1987). Abnormally high amounts of U reflect 1) the considerable content of U in the

Neoproterozoic shales and greywackes overlying the cave (2.9–6.1ppm) (Ungidos et al., 1997; Valladares et al., 2002) and 2) the aragonite composition of the samples.

According to Borsato et al. (2003), the ideal speleothem for dating should have enough U, no contamination of detritic Th and has remained a closed system with no remobilization or entrance of U or its decay products, especially ^{230}Th (Cherdyntsev 1971; Gascoyne et al. 1978; Ford and Williams 1989). According to Scholz and Hoffmann (2008) the breach of any of these criteria can generate anomalous ages.

Data obtained in COR-2 show three anomalous dates (Fig. 11, Table II). The first one (1) corresponds to the secondary calcite mosaic of Stage 1, which shows older ages than expected. Looking at the U concentration, the closest primary aragonite dated point is 2, with 14µg/g. Comparison of this value with the 5.5µg/g found in secondary calcites of point 1 indicates that there has been U-loss. According to reports, during recrystallyzation from aragonite to calcite the system behaves as semi-closed or open, with a redistribution of the large uranyl anion, unable to incorporate easily into calcite, with the consequent loss of U yielding false older ages (assuming that Th is immobile and there is no detrital contamination) (Ortega et al., 2005; Lachniet et al., 2012). Although older ages are expected due to U loss during open system conditions, the opposite can also occur (Ortega et al., 2005; Wassenburg et al., 2012; Scholz et al., 2014). Point number 5 corresponds to the calcite mosaic of Stage 2, so a similar situation as with that of point 1 would be expected. However, it is in stratigraphic concordance with the rest of ages and it seems that no U was lost, because the U content of the calcites (13.9 µg/g) was similar to the initial values of aragonite. In this case, during the transformation process the system remained closed, with an inheritance from the precursor mineral as described by Dominguez-Villar et al., 2017.

The second anomalous age is number 7, at the tip of the speleothem, with the oldest age of all samples. In this case, 100% aragonite (no recrystallization loss of U), with a concentration of U of 1.4μg/g, much lower than any of other aragonites dated (Table II). The fact that this sample is at the tip, he point where dripping water has been most present throughout time, with obvious dissolution features (Fig. 4d), suggests that there has been U-leaching related to dripping water (Scholz and Hoffmann, 2008). Moreover, the date immediately below (6) is also anomalous, so leaching of U can occur even at some distance from the surface in samples with high porosities. Dabous et al., 2000 described two events of U leaching in different stalagmites of Wadi Sannur cave, Egypt, related to well-documented higher rainfall rates in the eastern Egyptian desert.

6. Conclusions

Stalagmite COR-2 provided information about the geochemical behavior of an originally aragonite speleothem that underwent transformation to calcite in some parts. Detailed petrographical, mineralogical and geochemical analyses of the sample led to the following conclusions:

- Two stages of formation and transformation (Stage 1, Stage 2) were found to be repeated along the speleothem growth axis. Each stage was divided into several sub-stages (i.e. Stage 1a, 1b, 1c, etc.): precipitation of aragonite, cementation of micro-calcite crystals, transformation of aragonite into calcite and aragonite dissolution.
- The precipitation of aragonite was mainly controlled by CO_2 degassing rates with low discharge rates, indicated by the crystal morphology. Although the

Mg/Ca ratios in the parent waters may also have played a role in the formation of aragonite vs. calcite, as aragonite is generally found in caves in high-Mg host rocks.

- Calcite transformed the primary aragonite in the core, far from the surface of the speleothem. This implies the presence of a fluid in the pore system of the aragonite columnar crystals, where small calcite cement starts to precipitate, acting as a nucleus for transformation. According to the geochemical results, this fluid could have been the same aragonite-forming fluid, but diagenetically evolved, thus the entrance of waters with lower Mg/Ca ratios would not have been needed for calcite precipitation. In this case, it cannot be assured that aragonite and calcite formed under different climate conditions, but due to geochemical evolution of the fluid inside the speleothem.
- The secondary calcites were separated into groups of different crystal size and Mg-content, their spatial distribution and geochemistry indicate slight differences in the Mg/Ca ratio between the initial and the final composition of the recrystallizing fluid.
- The speleothem COR-2 shows two recrystallized areas yielding the same texture. During the recrystallizing processes of Stage 2b, the speleothem behaved as a closed-system, and during those of Stage 1b, as an open/semi-closed system.
- Presence of microcrystalline phases associated with dissolution processes (i.e. corrosion) not only occur on the surface of speleothems, but can occur in the inner part as a result of interaction between undersaturated waters with minerals.
- Two types of dating anomalies were found. The first which gives the oldest ages to the tip, is caused by leaching in parts of the speleothem most exposed to the

discharge of water. The second anomaly gives older ages to the secondary calcites than to the primary aragonite due to the fact U is incorporated in aragonite more easily than into calcite so there is U-loss during transformation. Both exaples assume that Th is immobile.

In summary, this paper highlights the complexity of speleothem diagenetic systems. Only after detailed mineralogical, petrological and geochemical studies is it possible to approach the processes involved in precipitation and transformation of speleothems, especially the originally aragonite speleothems, and in modification of the geochemical signals used for dating. These detailed studies become critical to a correct interpretation of paleo-environmental data based on speleothems.

Acknowledgements

This work was carried out under project CGL2014-54818-P from the Spanish Ministerio de Ciencia e Innovación. R. M-G is part of the "Laboratoire d'Excellence (LABEX)" TULIP (ANR-10-LABX-41) and the INTERREG POCTEFA ECTOPYR (no. EFA031/15). The authors are grateful to the valuable comments of Editor B. Jones, A. Košir and an anonymous reviewer who greatly improved the manuscript. James Cerne reviewed the English version of the manuscript.

References

Ahn, J-W., Kim, J-H., Park, H-S., Kim, J-A., Han, C., Kim, H., 2005. Synthesis of single phase aragonite precipitated calcium carbonate in Ca(OH)2-Na2CO3-NaOH reaction system. Korean Journal of Chemical Engineering 22, 852-856.

Alonso-Zarza, A.M., Martín-Pérez, A., 2008. Dolomite in caves: recent dolomite formation in oxic, non-sulfate environments. Castañar Cave, Spain. Sedimentary Geology 205, 160-164.

Alonso-Zarza, A.M., Martín-Pérez, A., Martín-García, R., Gil-Peña, I., Meléndez, A., Martínez-Flores, E., Hellstrom, J., Muñoz-Barco, P., 2011. Structural and host rock controls on the distribution, morphology and mineralogy of speleothems in the Castañar Cave (Spain). Geological Magazine 148, 211-225.

Alonso-Zarza A.M., Martín-García, R., Martín-Pérez, A., Olmeda-Zafrilla, P., Fernández-Amo, F.J., 2018. Origen y diagénesis de los espeleotemas de Cueva Masero, Monumento Natural Cuevas de Fuentes de León, Badajoz. Geogaceta 64, 119-122.

Auler, A.S., Smart, P.L., 2004. Rates of condensation corrosion in speleothems of semi-arid northeastern Brazil. Speleogenesis and Evolution of Karst Aquifers 2, 1-2.

Ayliffe, L.K., Veer, H.H., 1988. Uranium-series dating of speleothems and bones from Victoria Cave, Naracoorte, South Australia. Chemical Geology: Isotope Geoscience section 72, 211-234.

Bajo, P., Hellstrom, J., Haese, R., Frisia, S., Drysdale, R., Black, J., Woodhead, J., Borsato, A., Zanchetta, G., Wallace, M.W., Regattieri, E., 2016. "Cryptic" diagenesis and its implications for speleothem geochronologies. Quaternary Science Reviews 148, 17-28.

Baker, A., Flemons, I., Andersen, M.S., Coleborn, K., Treble, P.C., 2016. What determines the calcium concentration of speleothem-forming drip waters? Global and Planetary Change 143, 152-161.

Borsato, A., Quinif, Y., Bini, A., Dublyansky, Y., 2003. Open-system alpine speleothems: implications for U-series dating and paleoclimate reconstructions. Studi Trentini di Scienze Naturali: Acta Geologica 80, 71-83.

Cabrol, P., 1978. Contribution a l'etude du concretionnement carbonate des grottes du Sud de la France, morphologie, genese, diagenese, Université de Montpellier, Montpellier, 276 pp.

Caddeo, G.A., De Waele, J., Frau, F., Railsback, L.B., 2011. Trace element and stable isotope data from a flowstone in a natural cave of the mining district of SW Sardinia (Italy): evidence for Zn2+-induced aragonite precipitation in comparatively wet climatic conditions. International Journal of Speleology 40, 181-190.

Chave, K.E., 1964. Skeletal durability and preservation. Approaches to paleoecology. Wiley, New York, 377-387.

Chave, K.E., 1954. Aspects of the Biogeochemistry of Magnesium 2. Calcareous Sediments and Rocks. The Journal of Geology 62, 587-599.

Cherdyntsev, V.V., 1971. Uranium 234. Israel Programme for Scientific Translations, Jerusalem.

Cigna, A.A, 2005. Radon in caves. International Journal of Speleology 34, 1-18.

Coplen, T.B., 2007. Calibration of the calcite-water oxygen-isotope geothermometer at Devils Hole, Nevada, a natural laboratory. Geochimica et Cosmochimica Acta 71, 3948-3957.

Csoma, A.E., Goldstein, R.H., Pomar, L., 2006. Pleistocene speleothems of Mallorca: implications for palaeoclimate and carbonate diagenesis in mixing zones. Sedimentology 53, 213-236.

Dabous, A., Osmond, J., 2000. U/Th isotopic study of speleothems from the Wadi Sannur Cavern, Eastern Desert of Egypt. Carbonates and Evaporites 15, 1-6.

de Choudens-Sánchez, V., González, L.A., 2009. Calcite and aragonite precipitation under controlled instantaneous supersaturation: elucidating the role of $CaCO_3$ saturation state and Mg/Ca ratio on calcium carbonate polymorphism. Journal of Sedimentary Research 79, 363-376.

de Freitas, C.R., Schmekal, A., 2006. Studies of condensation/evaporation processes in the Glowworm Cave, New Zealand. International Journal of Speleology, 35, 75-81.

Delgado-Tejeda, V., 1988. Análisis de la vegetación en el paisaje natural de las Villuercas. Eria. 97-108.

Denniston, R.F., González, L.A., Asmerom, Y., Sharma, R.H., Reagan, M.K., 2000. Speleothem evidence for changes in Indian summer monsoon precipitation over the last ≈2300 years. Quaternary Research 53, 196-202.

Domínguez-Villar, D., Krklec, K., Cheng, H., Edwards, L. R. (2016). Dating an episode of paleo-condensation corrosion in Eagle Cave (Spain). In 24th International Karstological School" Classical Karst": Paleokarst.

Domínguez-Villar, D., Krklec, K., Pelicon, P., Fairchild, I.J., Cheng, H., Edwards, L.R., 2017. Geochemistry of speleothems affected by aragonite to calcite recrystallization - Potential inheritance from the precursor mineral. Geochimica et Cosmochimica Acta 200, 310-329.

Drysdale, R.N, Hellstrom, J.C., Zanchetta, G., Fallick, A.E., Sánchez Goñi, M.F., Couchoud, I., McDonald, J., Maas, R., Lohmann, G., Isola, I., 2009. Evidence for obliquity forcing of Glacial Termination II. Science 325, 1527-1531.

Duan, W., Cai, B., Tan, M., Liu, H., Zhang, Y., 2012. The growth mechanism of the aragonitic stalagmite laminae from Yunnan Xianren Cave, SW China revealed by cave monitoring. Boreas 41, 113-123.

Fairchild, I.J., Treble, P.C., 2009. Trace elements in speleothems as recorders of environmental change. Quaternary Science Reviews 28, 449-468.

Fairchild, I.J., Smith, C.L., Baker, A., Fuller, L., Spötl, C., Mattey, D., McDermott, F., E.I.M.F., 2006. Modification and preservation of environmental signals in speleothems. Earth-Science Reviews, 75, 105– 153.

Fernández-Cortés A, Sánchez-Moral S, Cañavera JC, Cuevas-González J, Cuezva S, Andreu JM, 2011. Variations in seepage water geochemistry induced by natural and anthropogenic microclimatic changes: Implications for speleothem growth conditions. Geodinamica Acta, 23, 1-13.Fernández-Díaz, L., Putnis, A., Prieto, M. and Putnis, C.V., 1996. The role of magnesium in the crystallization of calcite and aragonite in a porous medium. Journal of Sedimentary Research 66, 482-491.

Filipov, A., 1990. Formation conditions of aragonite in some caves from Pestera karst region, W. Phodopes. Ann. Sofia University, 162-173.

Folk, R.L., 1965. Some aspects of recrystallization in ancient limestones. In: L.C. Pray and R.C. Murray (Editors), Dolomitization and Limestone Diagenesis. A Symposium. SEMP Special Paper, Tulsa, Oklahoma, pp. 14-48.

Folk, R.L., 1974. The natural history of crystalline calcium carbonate effect of magnesium content and salinity. Journal of Sedimentary Petrology 44, 40-53.

Ford, D. C., Williams, P. W. 1989. Karst geomorphology and hydrology (Vol. 601). London: Unwin Hyman.

Frank, N., Braum, M., Hambach, U., Mangini, A., Wagner, G., 2000. Warm Period Growth of Travertine during the Last Interglaciation in Southern Germany. Quaternary Research, 38-48.

Frisia Bruni, S., Wenk, H.R., 1985. Replacement of aragonite by calcite in sediments from the San Cassiano Formation (Italy). Journal of Sedimentary Petrology 55, 159-170.

Frisia, S., 1996. Petrographic evidences of diagenesis in speleothems: some examples. Spéléocronos 7, 21-30.

Frisia, S., 2015. Microstratigraphic logging of calcite fabrics in speleothems as a tool for paleoclimate studies. International Journal of Speleology 44, 1-16.

Frisia, S., Borsato, A. 2010. Karst. In: Carbonates in continental settings: Facies, environments and processes (Eds A.M. Alonso-Zarza and L.H. Tanner), Elsevier, Oxford. pp. 269-318.

Frisia, S., Borsato, A., Fairchild, I.J., McDermott, F., Selmo, E.M., 2002. Aragonite-Calcite relationships in speleothems (Grotte de Clamouse, France): environment, fabrics, and carbonate geochemistry. Journal of Sedimentary Research 72, 687-699.

García-Guinea, J., Fernández-Cortes. A., Álvarez-Gallego, M., García-Antón, E., Casas-Ruiz, M., Blázquez-Pérez, D., Teijón, O., Cuezva, S., Correcher, V., Sánchez-Moral, S., 2013. Leaching of uranyl–silica complexes from the host metapelite rock favoring high radon activity of subsoil air: case of Castañar cave (Spain). Journal of Radionalytical and Nuclear Chemistry 298, 1567-1585.

Gascoyne, M., Ford, D.C., Schwarcz, H.P., 1978. Uranium series dating and stable isotope studies of speleothems. Part 1: Theory and techinques, Transactions British Cave Research Association, Buxton, pp. 91-112

Heiss J., Condon D. J., McLean N., Noble S. R., 2012. $^{238}U/^{235}U$ systematics in terrestrial uranium-earing minerals. Science 355 1610–1614.

Hellstrom, J., 2003. Rapid and accurate U/Th dating using parallel ion-counting multi-collector ICP-MS. Journal of Analytical Atomic Spectrometry 18, 1346-1351.

Hellstrom, J., 2006. U-Th dating of speleothems with high initial 230Th using stratigraphical constraint. Quaternary Geochronology 1, 289-295.

Hill, C.A., Forti, P. 1997. Cave minerals of the world. National Speleological Society, Huntsville, 463 pp.

Hoefs, J., 2009. Stable isotope geochemistry. Springer, Berlín, 201 pp.

Holland, H.D., Holland, H.J., Munoz, J.L., 1964. The coprecipitation of cations with $CaCO_3$-II. The coprecipitation of Sr^{+2} with calcite between 90° and 100°C. Geochimica et Cosmochimica Acta 28, 1287-1301.

Jones, B., 2017. Review of calcium carbonate polymorph precipitation in spring systems. Sedimentary Geology 353, 64-75.

Kaufman, A., Wasserburg, G.J., Porcelli, D., Bar-Matthews, M., Ayalon, A., Halicz, L., 1998. U-Th isotope systematics from the Soreq cave, Israel and climatic correlations. Earth and Planetary Science Letters 156, 141-155.

Kaufmann, G., 2003. Stalagmite growth and palaeo-climate: the numerical perspective. Earth and Planetary Science Letters 214, 251-266.

Kim, S.-T., O'Neil, J.R., Hillaire-Marcel, C., Mucci, A., 2007. Oxygen isotope fractionation between synthetic aragonite and water: Influence of temperature and Mg2+ concentration. Geochimica et Cosmochimica Acta 71, 4704-4715.

Lachniet, M.S., Bernal, J.P., Asmerom, Y., Polyak, V., 2012. Uranium loss and aragonite-calcite age discordance in a calcitized aragonite stalagmite. Quaternary Geochronology 14, 26-37.

Lario, J., Sánchez-Moral, S., Cuezva, S., Taborda, M., Soler, V., 2006. High 222Rn levels in a show cave (Castañar de Ibor, Spain): Proposal and application of management measures to minimize the effects on guides and visitors. Atmospheric Environment 40, 7395–7400.

Lippmann, F., 1973. Sedimentary carbonate minerals. Springer-Verlag, Berlin, 228 pp.

Martín-García, R., 2012. La diagénesis de los espeleotemas de las Cuevas de Castañar de Ibor, Cáceres y Basajaún Etxea, Navarra. Implicaciones para el estudio del registro paleoclimático. PhD Thesis, Universidad Complutense de Madrid, Madrid, 194 pp.

Martín-García, R., Alonso-Zarza, A.M., Martín-Pérez, A., 2009. Loss of primary texture and geochemical signatures in speleothems due to diagenesis: Evidences from Castañar Cave, Spain. Sedimentary Geology 221, 141-149.

Martín-García, R., Alonso-Zarza, A.M., Martín-Pérez, A., Schröder-Ritzrau, A., Ludwig, T., 2014. Relationships between colour and diagenesis in the aragonite-calcite speleothems in Basajaún Etxea cave, Spain. Sedimentary Geology 312, 63-75.

Martín-García, R., Martín-Pérez, A. and Alonso-Zarza, A.M., 2011. Weathering of host rock and corrosion over speleothems in Castañar cave, Spain: an example of a complex meteoric environment. Carbonates and Evaporites 26, 83-94.

Martín-Pérez, A., Martín-García, R., Alonso-Zarza., A.M., 2012. Diagenesis of a drapery speleothem from Castañar Cave: from dissolution to dolomitization. International Journal of Speleology 41, 251-266.

McMillan, E.A., Fairchild, I.J., Frisia, S., Borsato, A., McDermott, F., 2005. Annual trace element cycles in calcite–aragonite speleothems: evidence of drought in the western Mediterranean 1200–1100 yr BP. Journal of Quaternary Science 20, 423-433.

Mook, W.G., Bommerson, J.C., Staverman, W.H., 1974. Carbon isotope fractionation between dissolved bicarbonate and gaseous carbon dioxide. Earth and Planetary Science Letters 22, 169-176.

Neymark, L.A. 2011. Potential of alpha-recoil on uranium-series dating of calcrete. Chemical Geology 282, 98-112

Ninyerola, M., Pons, X., Roure, J.M. (Editors), 2005. Atlas Climático digital de la Península Ibérica. Metodología y aplicaciones en bioclimatología y geobotánica. Universidad Autónoma de Barcelona, Bellaterra.

Ortega, R., Maire, R., Devès, G., Quinif, Y., 2005. High-resolution mapping of uranium and other trace elements in recrystallized aragonite–calcite speleothems from caves in the Pyrenees (France): Implication for U-series dating. Earth and Planetary Science Letters 237, 911-923.

Perdikouri, C., Kasioptas, A., Putnis, C.V., Putnis, A. 2008. The effect of fluid composition on the mechanism of the aragonite to calcite transition. Mineralogical Magazine 72, 111-114.

Perrin, C., Prestimonaco, L., Servelle, G., Tilhac, R., Maury, M., Cabrol, P., 2014. Aragonite-calcite speleothems: identifying original and diagenetic features. Journal of Sedimentary Research 84, 245-269.

Pingitore, N.E., 1976. Vadose and phreatic diagenesis; processes, products and their recognition in corals. Journal of Sedimentary Petrology 46, 985-1006.

Quinif, Y., 1987. Concentrations anomales en uranium dans les stalagmites (gouffre de la Pierre de Saint-Martin, Pyrénées, France). Bulletin de la Société Belge de Géologie 96, 121-128.

Railsback, L.B., Brook, G.A., Chen, J., Kalin, R., Fleisher, C.J., 1994. Environmental controls on the petrology of a late Holocene speleothem from Botswana with annual layers of aragonite and calcite. Journal of Sedimentary Research 64, 147-155.

Reeder, R.J., Nugent, M., Lamble, G.M., Tait, C.D., Morris, D.E., 2000. Uranyl incorporation into calcite and aragonite: XAFS and luminiscence studies. Environmental Science and Technology 34, 638-644.

Reid, R.P., Macintyre, I.G., 1998. Carbonate recrystallization in shallow marine environments: A widespread diagenetic process forming micritized grains. Journal of Sedimentary Research 68, 928-946 Part A.

Rodríguez-Berriguete, Á., Alonso-Zarza, A.M., Martín-García, R., Cabrera, M.C., 2018. Sedimentology and geochemistry of a human-induced tufa deposit: Implications for palaeoclimatic research. Sedimentology 65, 2253-2277.

Romanek, C.S., Grossman, E.L., Morse, J.W., 1992. Carbon isotopic fractionation in synthetic aragonite and calcite: Effectsof temperature and precipitation rate. Geochimica et Cosmochimica Acta 56, 419-430.

Romanov, D., Kaufmann, G., Dreybrodt, W., 2008. Modeling stalagmite growth by first principles of chemistry and physics of calcite precipitation. Geochimica et Cosmochimica Acta 72, 423-437.

Rossi, C., Lozano, R.P., 2016. Hydrochemical controls on aragonite versus calcite precipitation in cave dripwaters. Geochimica et Cosmochimica Acta 192, 70-96.

Rowling, J., 2004. Studies on aragonite and its occurrence in caves, including New South Wales Caves. Journal and Proceedings of the Royal Society of New South Wales, 137: 123-149.

Sánchez-Moral, S., Cuezva, S., Lario, J., Taborda-Duarte, M., 2006. Hydrochemistry of karstic waters in a low-energy cave (Castañar de Ibor, Spain). In: J.J. Durán, B. Andreo and F. Carrasco (Editors), Karst, cambio climático y aguas subterráneas. Hidrogeología y aguas subterráneas. IGME, Madrid, pp. 339-347.

Sánchez-Moral, S. 2015. Convenio de colaboración entre la Consejería de Agricultura, Desarrollo Rural, Medio Ambiente y Energía de la Junta de Extremadura y la Agencia Estatal Consejo Superior de Investigaciones Científicas para el seguimiento ambiental y el estudio geológico del Monumento Natural "Cueva de Castañar". Informe final. 113 pp.

Sandberg, P.A., Hudson, J.D., 1983. Aragonite relic preservation in Jurassic calcite-replaced bivalves. Sedimentology 30, 879–892

Scholz, D., Hoffmann, D., 2008. ^{230}Th/U-dating of fossil corals and speleothems. Eiszeitalter und Gegenwart. Quaternary Science Journal 57, 52-76.

Scholz, D., Tolzmann, J., Hoffmann, D.L., Jochum, K.P., Spötl, C., Riechelmann, D.F.C., 2014. Diagenesis of speleothems and its effect on the accuracy of 230Th/U-ages. Chemical Geology 387, 74-86.

Spötl, C., Mangini, A., Frank, N., Eichstadter, R., Burns, S.J., 2002. Start of the last interglacial period at 135 ka: Evidence from a high Alpine speleothem. Geology 30, 815-818.

Spötl, C., Scholz, D., Mangini, A., 2008. A terrestrial U/Th-dated stable isotope record of the Penultimate Interglacial. Earth and Planetary Science Letters 276, 283-292.

St Pierre, E., Zhao, J.-x., Reed, E., 2009. Expanding the utility of Uranium-series dating of speleothems for archaeological and palaeontological applications. Journal of Archaeological Science 36, 1416-1423.

Tucker, M.E., Wright, P.V., 1990. Carbonate sedimentology. Blackwell Publishing, Oxford. 496 pp.

Ugidos, J.M., Armenteros, I., Barba, P., Valladares, M.I., Colmenero, J.R., 1997. Geochemistry and petrology of recycled orogen-derived sediments: a case study

from Upper Precambrian siliciclastic rocks of the Central Iberian Zone, Iberian Massif, Spain. Precambrian Research 84, 163-180.

Valladares, M.I., Ugidos, J.M., Barba, P., Colmenero, J.R., 2002. Contrasting geochemical features of the Central Iberian Zone shales (Iberian Massif, Spain): implications for the evolution of Neoprpterozoic-Lower Cambrian sediments and their sources in other peri-Gondwanan areas. Tectonophysics 352, 121-132.

van Calsteren, P. and Thomas, L., 2006. Uranium-series dating in natural enviroment science. Earth-Science Reviews 75, 155-175.

Wassenburg, J.A., Immenhauser, A., Richter, D.K., Jochum, K.P., Fietzke, J., Deininger, M., Goos, M., Scholz, D., Sabaoui, A. 2012. Climate and cave control on Pleistocene/Holocene calcite-to-aragonite transitions in speleothems from Morocco: elemental and isotopic evidence. Geochimica et Cosmochimica Acta 92, 23-47.

Wassenburg, J.A., Scholz, D., Jochumb, K.P., Cheng, H., Ostere, J., Immenhauser, A., Richter, D.K., Häger, T., Jamieson, R.A., Baldini, J.U.L., Hoffmann, D., Breitenbach, S.F.M., 2016. Determination of aragonite trace element distribution coefficients from speleothem calcite-aragonite transitions. Geochimica et Cosmochimica Acta 190, 347-367.

Woo, K.S., Choi, D.W., 2006. Calcitization of aragonite speleothems in limestone caves in Korea: Diagenetic process in a semiclosed system In: R.S. Harmon and C. Wicks (Editors), Perspectives on karst geomorphology, hydrology, and geochemistry. A tribute volume to Derek C. Ford and William B. White. Geological Society of America Special Paper. Geological Society of America, Boulder, Colorado, pp. 297-306.

Zhang, H., Cai, Y., Tan, L., Qin, S., An, Z., 2014. Stable isotope composition alteration produced by the aragonite-to-calcite transformation in speleothems and implications for paleoclimate reconstructions. Sedimentary Geology 309, 1-14.

Zhang, Y. and Dawe, R.A., 2000. Influence of Mg^{2+} on the kinetics of calcite precipitation and calcite crystal morphology. Chemical Geology 163, 129-138.

FIGURE CAPTIONS

Fig. 1. A) Location map of the cave. B) Geological profile of Ibor anticline and location of the cave within. C) Sampling site in Corales room. D) Aspect of the studied stalagmite.

Fig 2. Inner aspect of the studied stalagmite. f1 to f3 refer to the different fabrics described in the text. A) Elongated columnar aragonite crystals with some dissolution features between the crystals. Plain-polarized light. B) Calcite mosaic with aragonite relicts. Cross-polarized light. C) Microcrystalline aragonite between primary aragonite (top) and secondary calcite mosaic (bottom). Plain-polarized light.

Fig. 3. Mineralogical composition of 10 selected points. Numbers 1, 2 and 6 to 8 are secondary calcites with up to 50% aragonite relicts.

Fig. 4. Optical and SEM images of elongated columnar aragonite crystals of COR-2. (A) Aragonite fans intercrossing each other. Plain-polarized light. (B) SEM image of an aragonite crystal tip with square termination. (C) Calcite microcrystals growing as cement in the porosity between the aragonite crystals, SEM image. (D) Plain-polarized light of the speleothem tip formed by elongated columnar aragonite crystals with abundant dissolution features and enlarged porosity.

Fig. 5. Optical and SEM images of calcite mosaic of COR-2. (A) Mosaic of large and small calcite crystals with aragonite relicts. Plain-polarized light. Notice the higher presence of relicts in the larger crystals. (B) SEM image of a large calcite surrounded by the smaller calcites in the contact with the microcrystalline aragonite (top left). (C) Aragonite relicts inside calcite crystals follow the same direction as the primary elongated columnar aragonite crystals. Plain-polarized light. (D) Calcite crystals of different sizes with variable proportion of relicts. Usually the edges of the calcite crystals are relict-free. Cross-polarized light.

Fig. 6. Microcrystalline aragonite. (A) Aspect of the with powdery patches in the speleothem section. (B) Microcrystalline aragonite detached from the surfaces of the columnar aragonite crystals. Notice that the semi-dissolution transforms the columnar crystals into needles by favored dissolution along the splitting surfaces. SEM image. (C) Close up view of the aragonite crystals covered with microcrystals. Some parts of the primary crystals are still distinguishable. Plain-polarized light. (D) Microcrystalline aragonite showing the original disposition of the primary aragonites. Plain-polarized light.

Fig. 7. Formation and transformation stages of COR-2. Stage 1: 1a) formation of a fully aragonite stalagmite. 1bi) multiple nucleation sites started the recrystallization process. The number and position of sites is unknown. 1bf) the final product of the recrystallization is a calcite mosaic in the core of the speleothem. After this sub-stage the aragonite appears as a rim. 1c) Partial dissolution of the aragonite in the contact with the secondary calcite mosaic. Stage 2: 2a) a new aragonite stalagmite grows on the previous stage. 2bi, 2bf) same situation as in Stage 1. 2c) identical to 1c but the partial dissolution also affected the aragonite in the contact between Stage 1 and 2.

Fig. 8. Results of microprobe analyses of individual crystals of calcite and aragonite. Large and small calcites are separated, aragonite englobes all the textures found (elongated columnar, relicts and microcrystals).

Fig. 9. Oxygen and carbon stable isotope records, and Ca and Mg contents of COR-2 along the central axis of the speleothem in calcite mosaic of Stage 1b.

Fig. 10. Oxygen and carbon stable isotope records, and Ca, Mg and Sr contents of COR-2 in a profile perpendicular to the growth axis. Small calcite mosaic present the lightest $\delta^{13}C$ and the highest contents of Mg.

Fig. 11. Dated points of the sample. Anomalous results in red.

Fig. 12. Diagenetic evolution of fluids inside the porosity of the speleothem. As calcite precipitates, the system is depleted in Ca and Mg/Ca ratio arises provoking the precipitation of Mg-rich calcites with a smaller size due to "poisoning". SI decreases until the fluids are become aggressive, dissolving the aragonite. The incorporation of the heavy $\delta^{13}C$ isotope in the minerals, give the lightest values to the last phases to form.

Table I. Mean % mol of carbonates of selected elements in calcites and aragonites of sample COR-2.

Table II. U–Th activity ratio and age data for seven speleothem samples. Samples analysed using the procedure of Hellstrom (2003). The numbers in round brackets are fully propagated 95 % uncertainties taking into account long-term reproducibility of powdered standard materials. ($^{230}Th/^{238}U$) and ($^{234}U/^{238}U$) are determined using a ^{229}Th–^{233}U mixed spike calibrated against a Harwell uraninite (HU–1) solution. Age is calculated assuming an initial $^{230}Th/^{232}Th$ activity ratio of 1.5±1.5 using equation 1 of Hellstrom (2006), although the effect of initial ^{230}Th is negligible in this case. $^{234}U/^{238}U)i$ is calculated using ($^{234}U/^{238}U$) and the corrected age.

Table 1

Mineralogy	Texture	No. Samples	$CaCO_3$	$MgCO_3$	$SrCO_3$	$FeCO_3$	$MnCO_3$	$BaCO_3$
Ar	Coulumnar elongated	13	99,831	0,007	0,015	0,035	0,041	0,071
Ar	Relics	16	99,778	0,004	0,009	0,040	0,099	0,069
Ar	Microcrystalline	4	99,945	0,000	0,022	0,000	0,033	0,000
Cc	Large euhedral	23	99,771	0,120	0,015	0,033	0,023	0,013
Cc	Small euhedral	34	98,761	1,066	0,001	0,094	0,044	0,025

Table 2

Sample	Mineralogy /Fabric	U (µg/g)	$^{230}Th/^{238}U$	$^{234}U/^{238}U$	$^{232}Th/^{238}U$	$^{230}Th/^{232}Th$	Age (ka)	$(^{234}U/^{238}U)i$
COR-2.1	Calcite mosaic	5.477	1.470 (05)	2.736 (07)	0.000042 (01)	34935.4	76.324 (0.8)	3.156 (07)
COR-2.2	Ray aragonite	14.014	1.041 (11)	2.716 (05)	0.000002 (03)	566773.2	49.797 (0.6)	2.976 (06)
COR-2.3	Ray aragonite	9.863	1.113 (05)	2.903 (06)	0.000002 (01)	526205.4	49.717 (0.3)	3.190 (06)
COR-2.4	Microcrystallyne aragonite	13.951	1.065 (07)	2.838 (04)	0.000007 (01)	163774	48.482 (0.4)	3.108 (05)
COR-2.5	Calcite mosaic	13.526	0.982 (03)	2.676 (05)	0.000003 (01)	331457.8	47.311 (0.2)	2.917 (05)
COR-2.6	Ray aragonite	8.826	1.178 (06)	2.749 (05)	0.000008 (01)	146321.7	57.062 (0.4)	3.056 (06)
COR-2.7	Ray aragonite	1.408	2.928 (12)	3.036 (07)	0.001101 (40)	2659.4	195.44 (2.1)	4.542 (18)

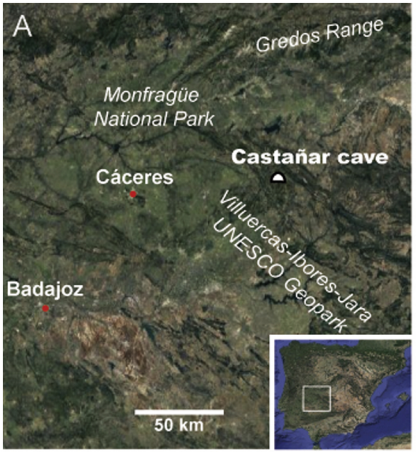
A
Gredos Range
Monfragüe
National Park
Castañar cave
Cáceres
Villuercas-Ibores-Jara
UNESCO Geopark
Badajoz
50 km


C


D
5 cm

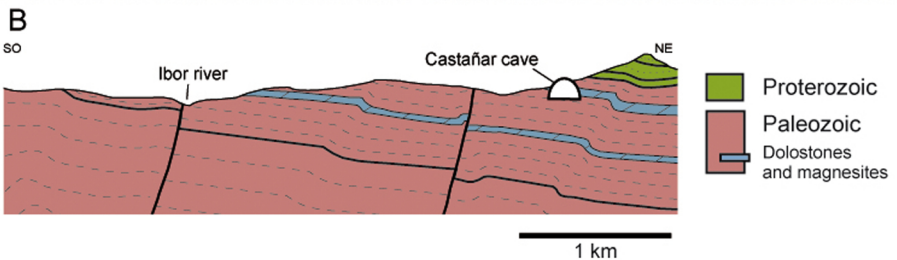
B
SO
Ibor river
Castañar cave
NE
Proterozoic
Paleozoic
Dolostones
and magnesites
1 km

Figure 1

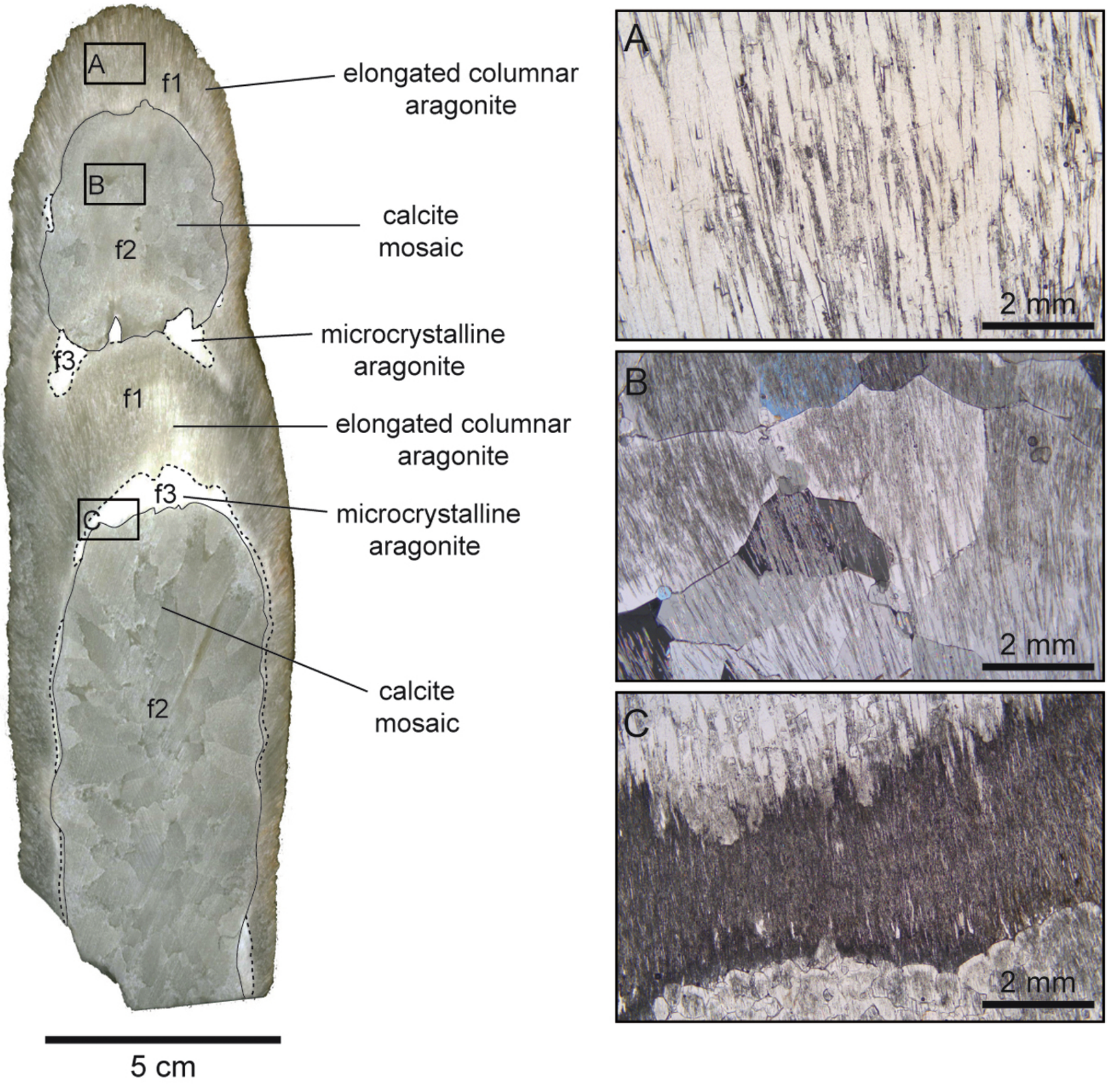
A
f1
elongated columnar aragonite
B
calcite mosaic
f2
microcrystalline aragonite
f3
f1
elongated columnar aragonite
f3
C
microcrystalline aragonite
calcite mosaic
f2
5 cm
A
2 mm
B
2 mm
C
2 mm

Figure 2

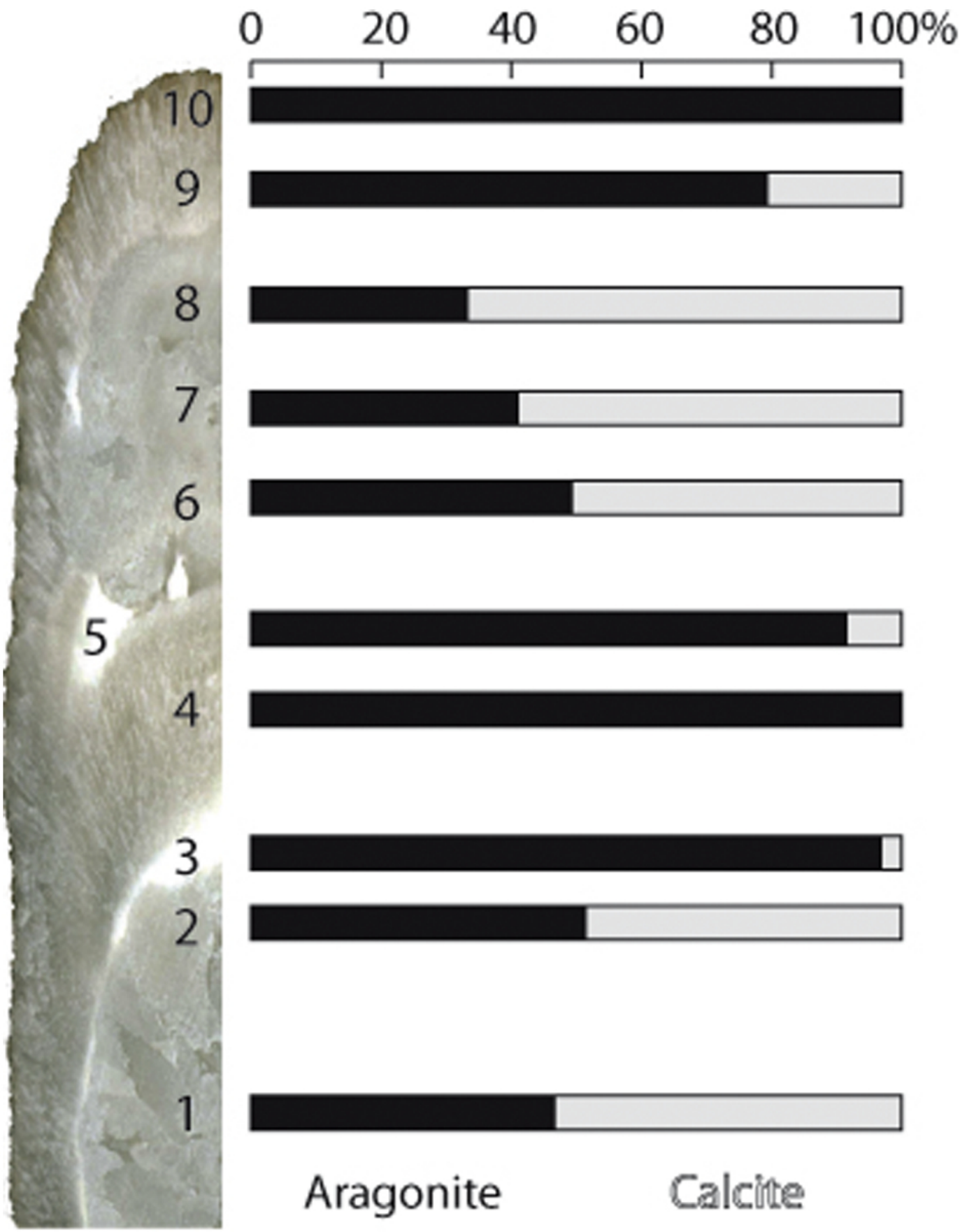

Figure 3

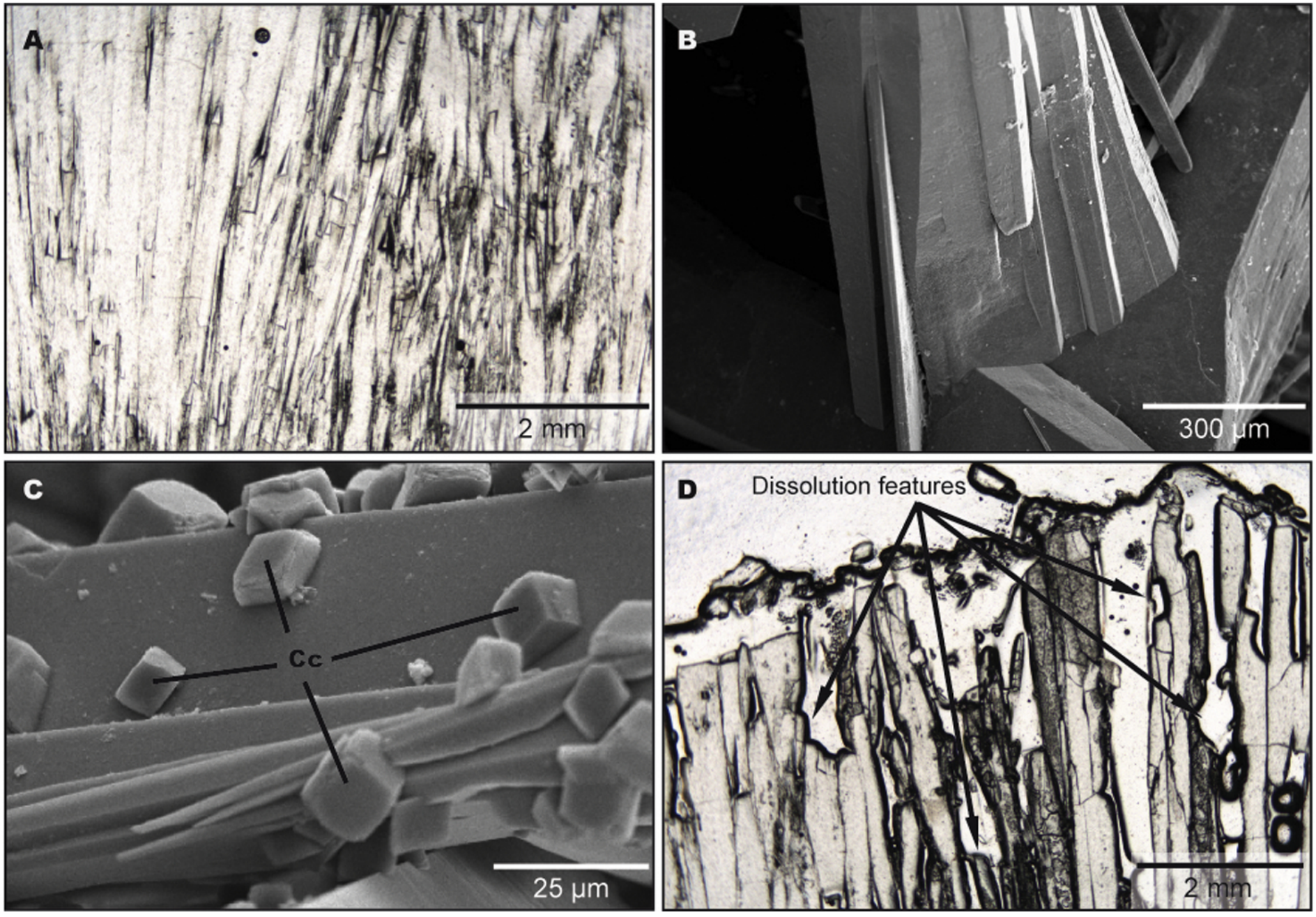

Figure 4

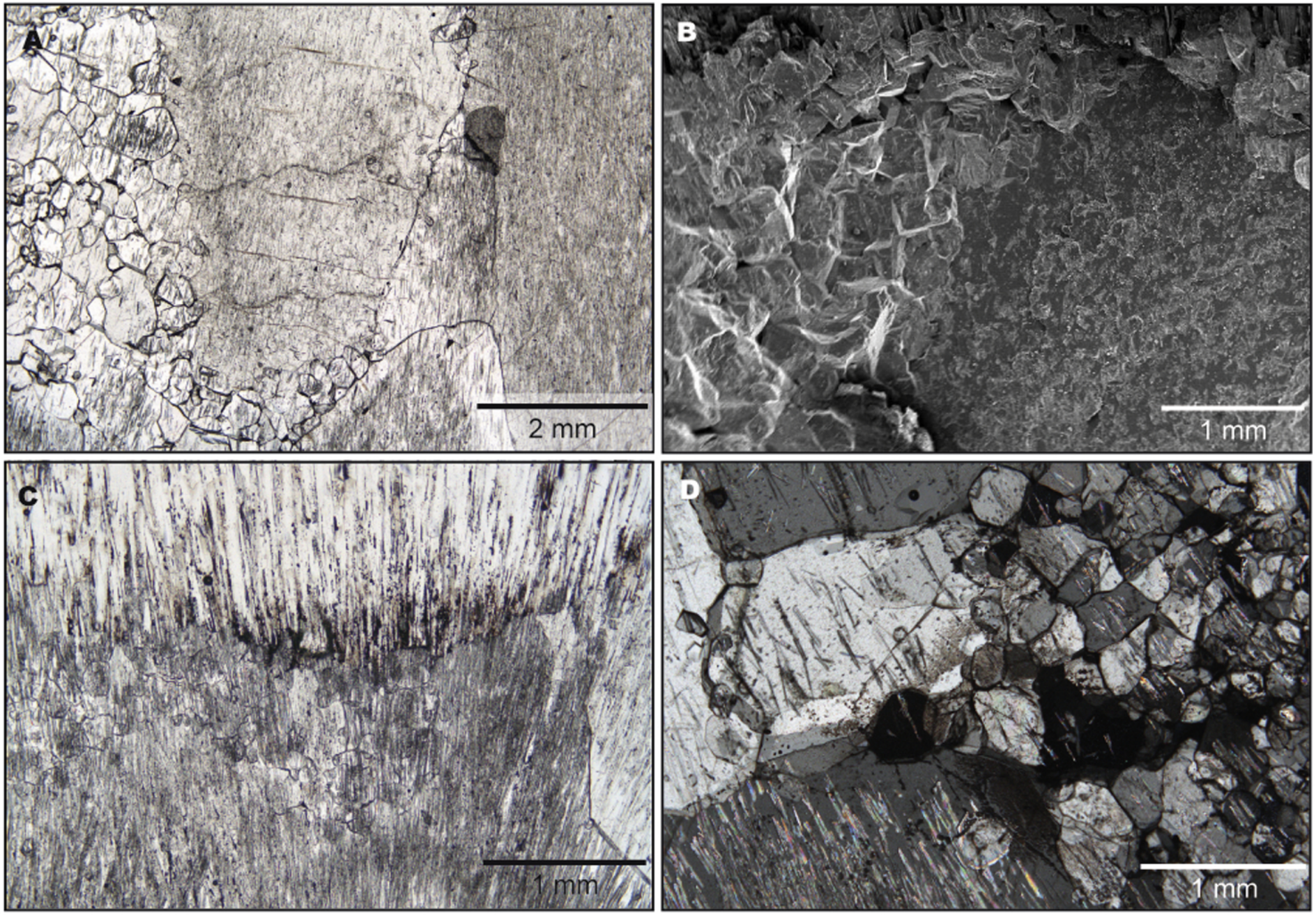

Figure 5

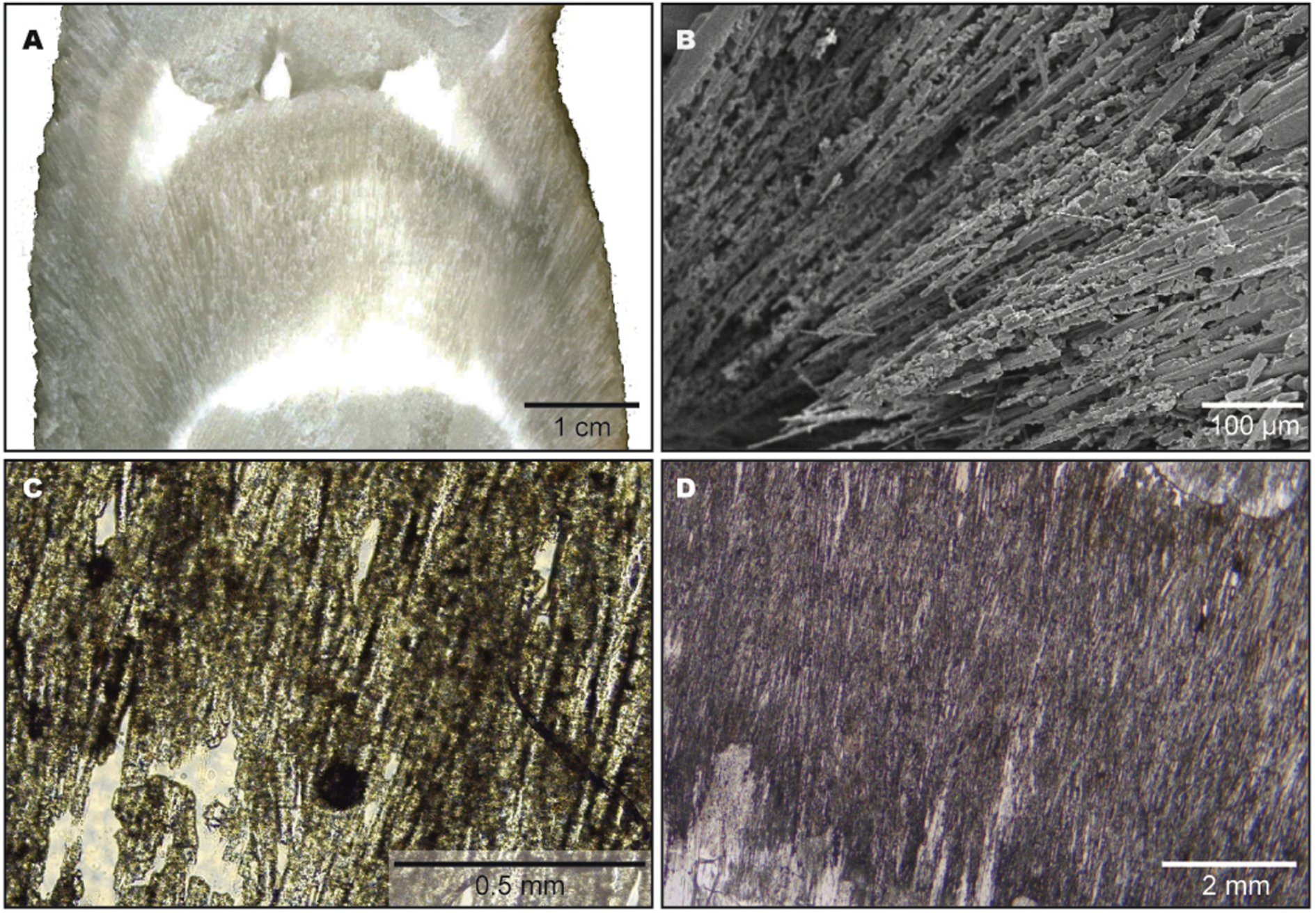

Figure 6

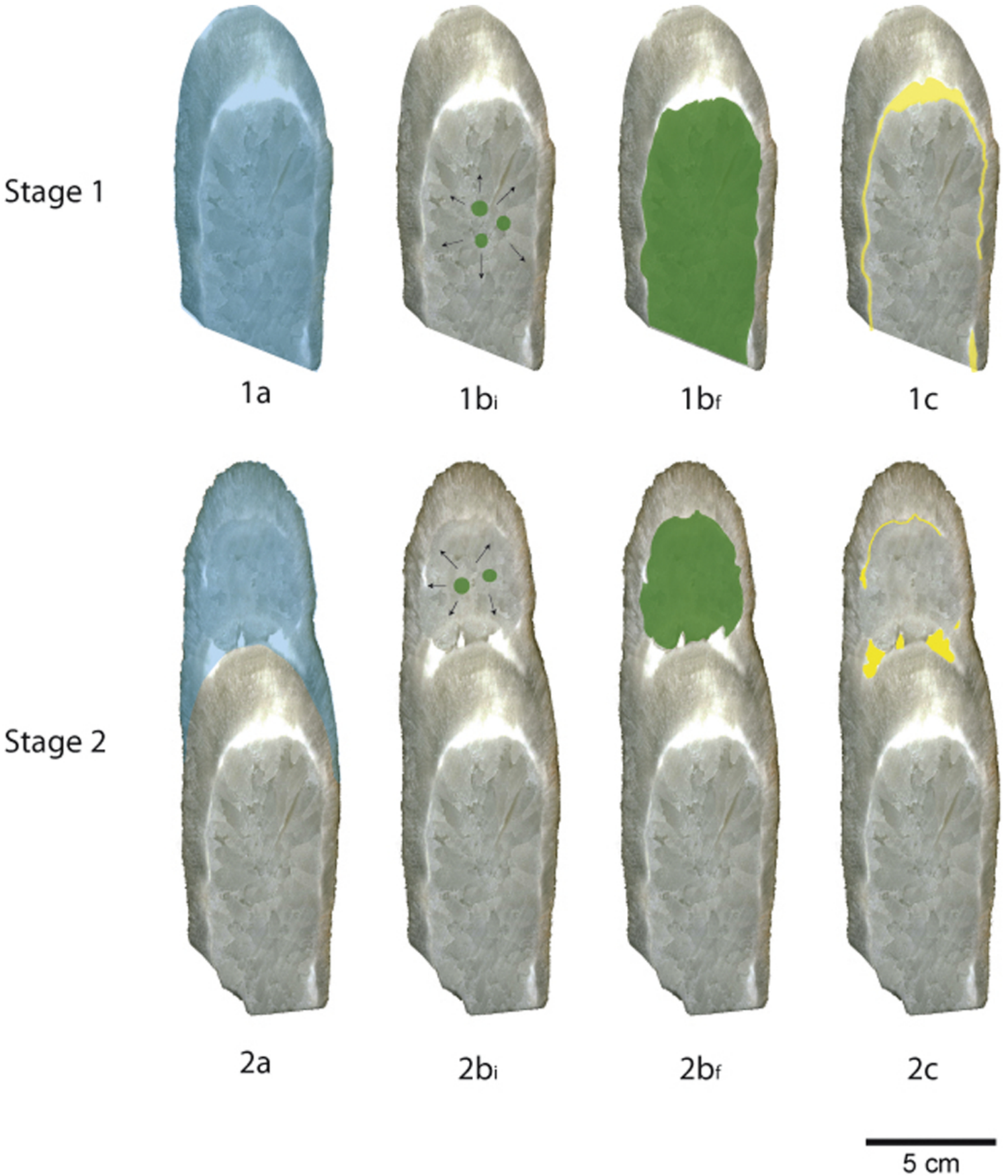

Figure 7

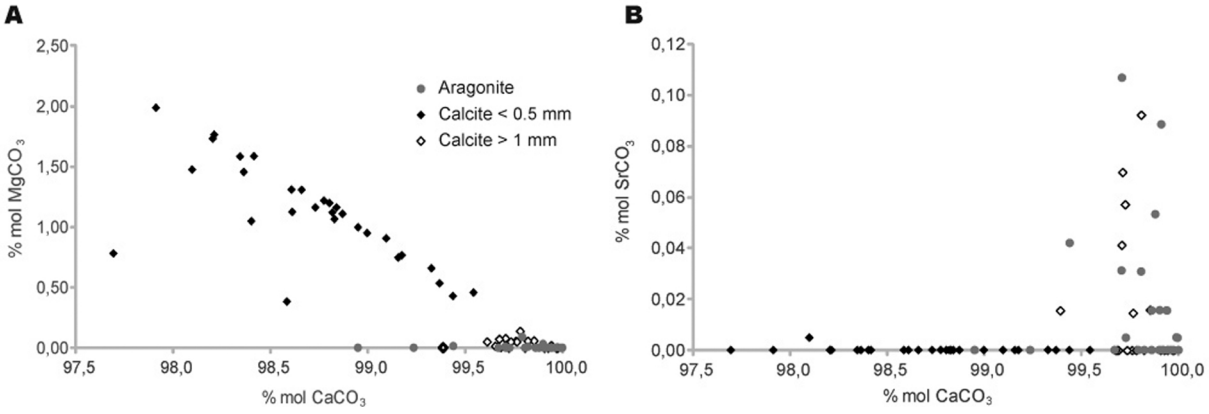
A
2,50
2,00
1,50
1,00
0,50
0,00
% mol MgCO3
97,5
98,0
98,5
99,0
99,5
100,0
% mol CaCO3
Aragonite
Calcite < 0.5 mm
Calcite > 1 mm
B
0,12
0,10
0,08
0,06
0,04
0,02
0,00
% mol SrCO3
97,5
98,0
98,5
99,0
99,5
100,0
% mol CaCO3

Figure 8

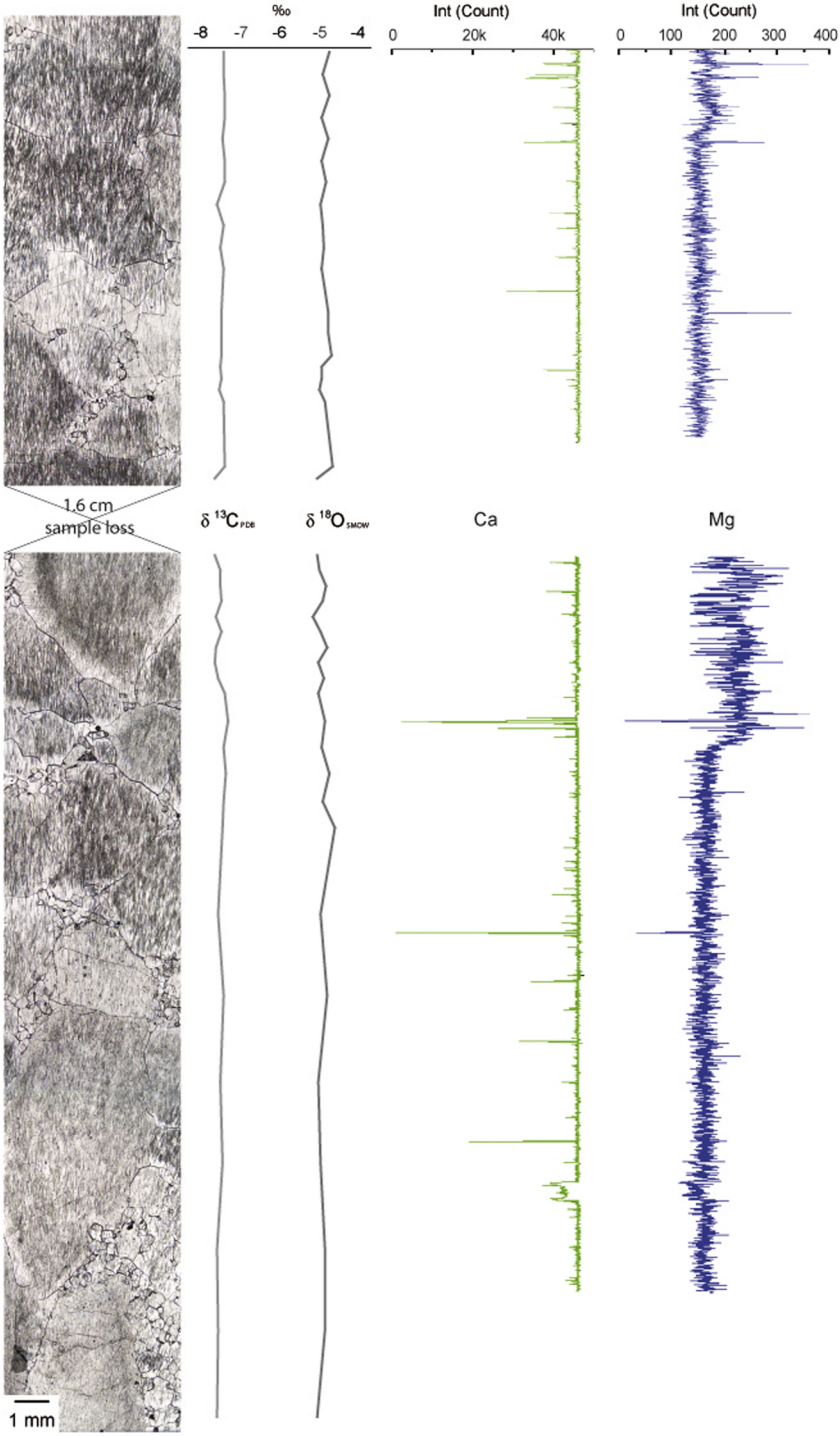
‰
-8
-7
-6
-5
-4
Int (Count)
0
20k
40k
Int (Count)
0
100
200
300
400
1.6 cm
sample loss
δ 13C PDB
δ 18O SMOW
Ca
Mg
1 mm

Figure 9

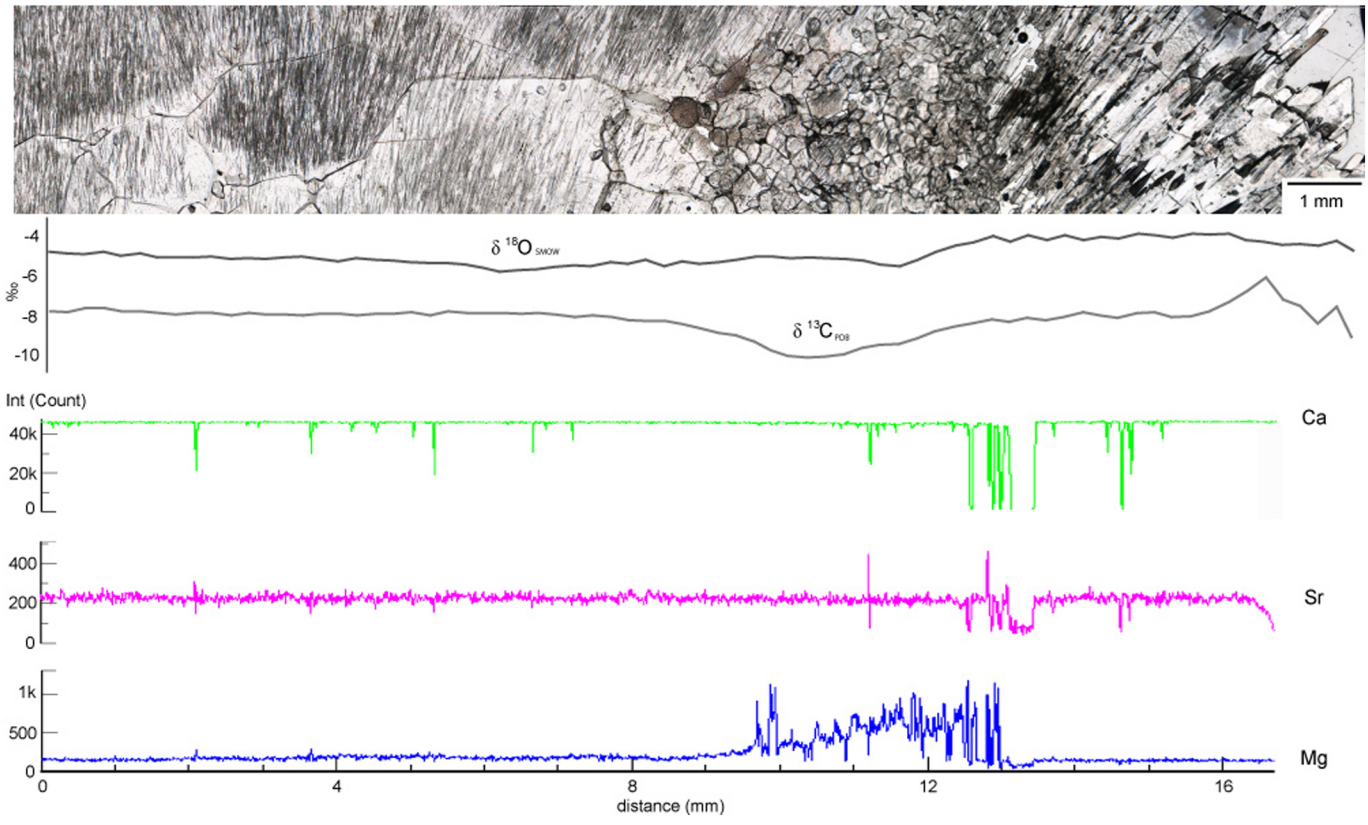
1 mm
δ 18O SMOW
δ 13C PDB
‰
-4
-6
-8
-10
Int (Count)
Ca
Sr
Mg
40k
20k
0
400
200
0
1k
500
0
0
4
8
12
16
distance (mm)

Figure 10

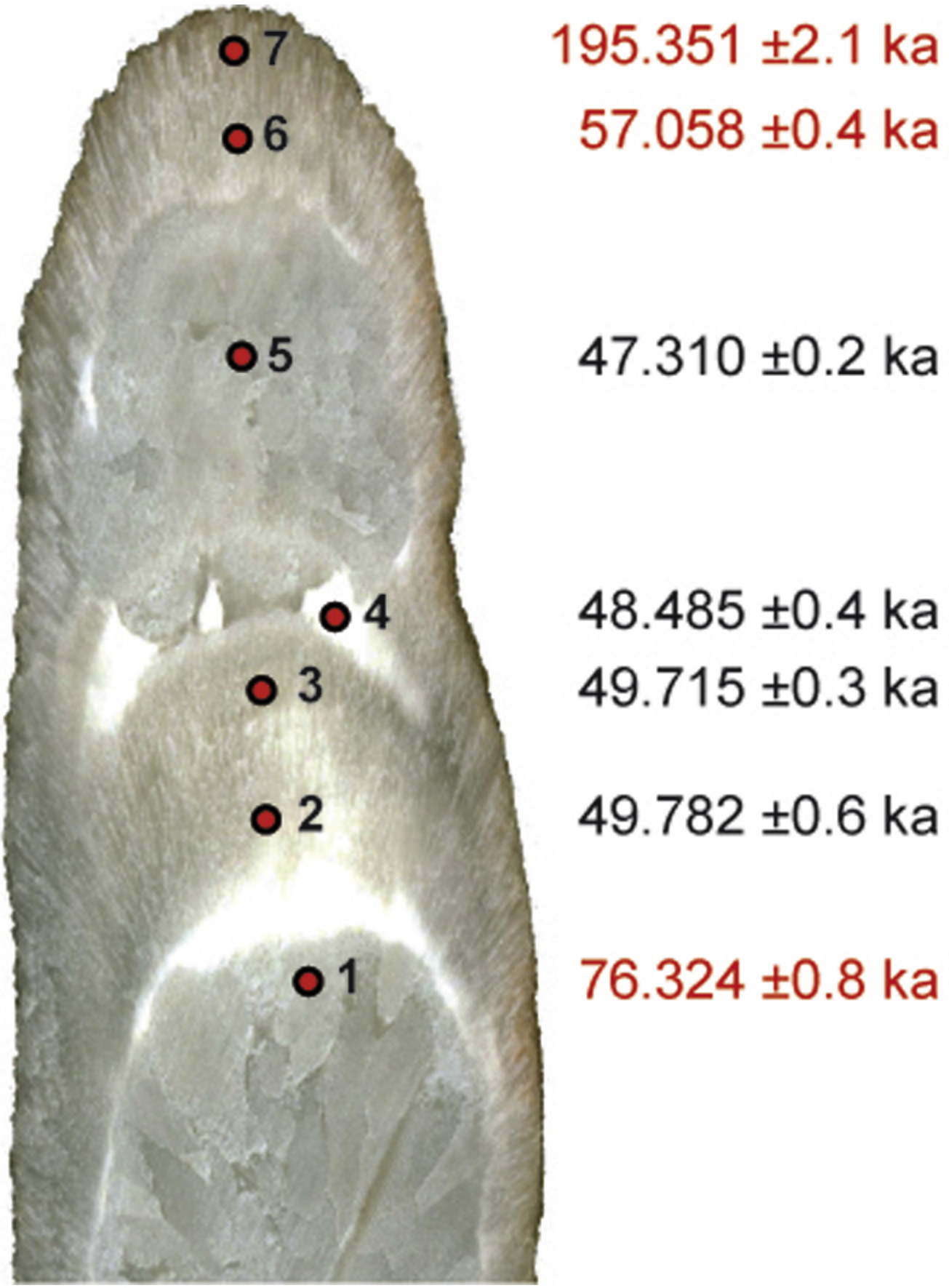
7
6
5
4
3
2
1
195.351 ±2.1 ka
57.058 ±0.4 ka
47.310 ±0.2 ka
48.485 ±0.4 ka
49.715 ±0.3 ka
49.782 ±0.6 ka
76.324 ±0.8 ka

Figure 11

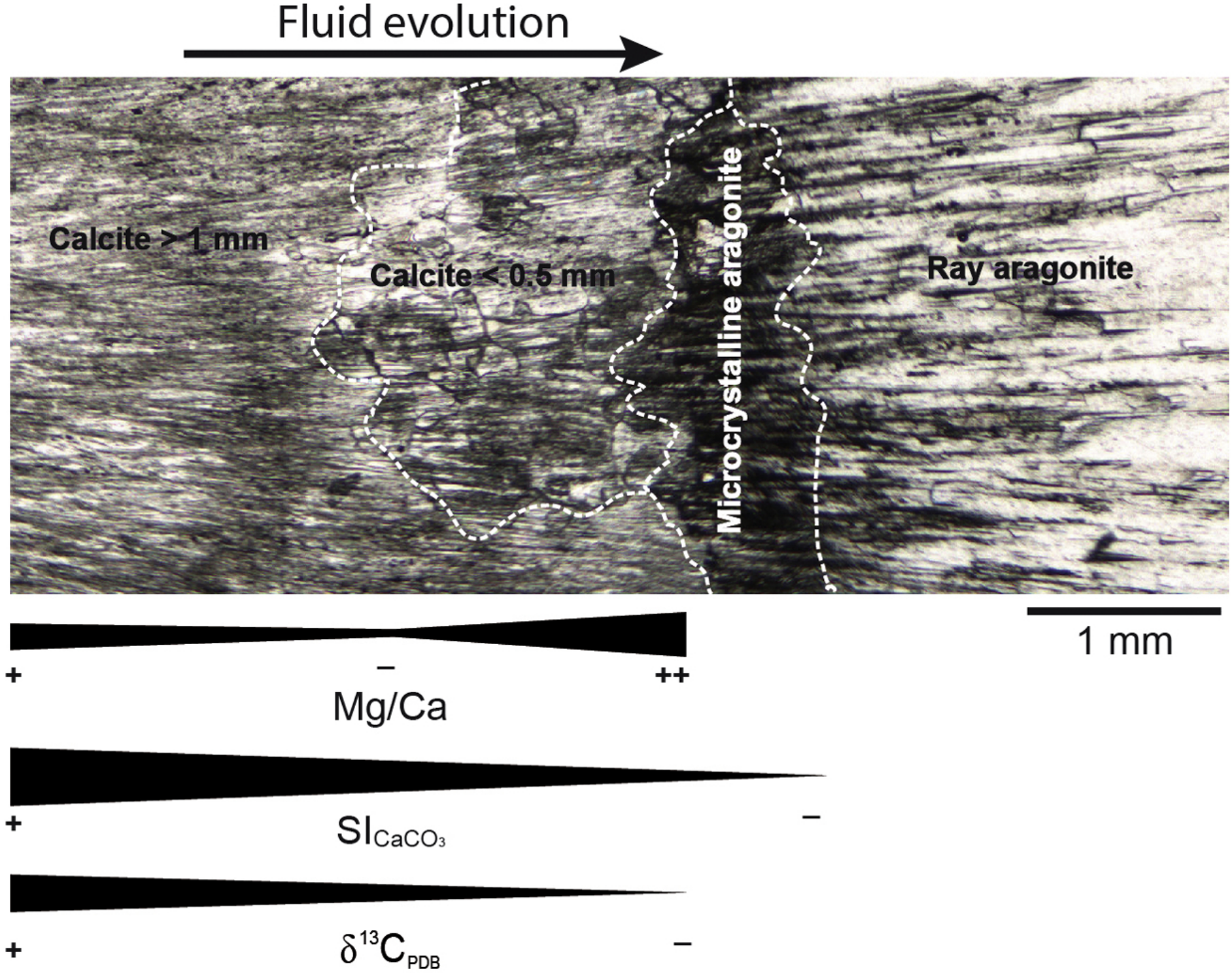
Fluid evolution
Calcite >1 mm
Calcite < 0.5 mm
Microcrystalline aragonite
Ray aragonite
1 mm
+
–
++
Mg/Ca
+
–
SICaCO3
+
–
δ13CPDB

Figure 12